

Supporting Information

May the *Oxa*-Michael Reaction of 2-Trifluoromethacrylic Acid Lead to Original Fluorinated Polyester?

Minh-Loan Tran-Do, Nadim Eid, Cédric Totée, Olinda Gimello, Bruno Améduri*

Institut Charles Gerhardt, Univ. Montpellier, CNRS, ENSCM, Montpellier, France. E-mail: bruno.ameduri@enscm.fr

Polymerisation set-up

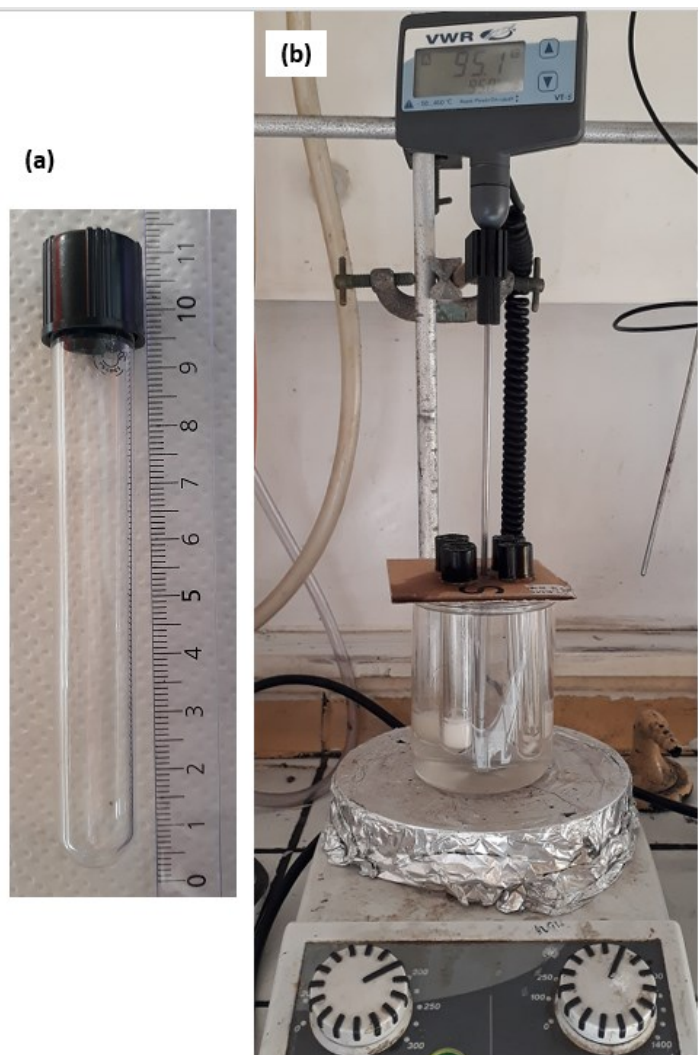


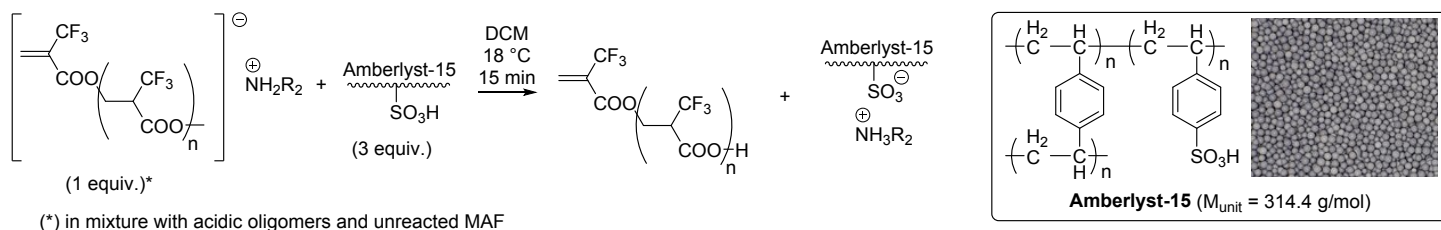
Figure S1: (a) Reaction tube; (b) Reactions set up for 4 reactions in 1.4 gram scale.

Polymerisation procedure. In a reaction tube (Figure S1a) equipped with a magnetic stirrer, were introduced MAF and additive. The tube was purged under N_2 before being sealed and immersed into an oil bath heated at the requested temperature. The polymerisation was stopped after 24 hrs by cooling the tube to room temperature. Immersion of the tube enabled to prevent the sublimation of MAF. Compared to round bottom flasks, the tubes allow to easily proceed simultaneous several (4 in the case of our experiments) reactions in 1.4 gram scale (Figure S1b). For reactions with amines, a filtration over Amberlyst 15 was necessary to remove the produced ammonium (Scheme S1 & Figure S2). A subsequent sublimation at 60 - 70 °C under reduced pressure was achieved to remove the unreacted MAF and afford oligoMAF as a yellowish and translucent gel.

Polymerisation work-up

With amines : ammonium removal with Amberlyst 15

Amberlyst 15 is a crosslinked ion exchange resin bearing $-\text{SO}_3\text{H}$ functions^{1,2} which are able to trap the ammonium cations and protonate then the carboxylate to regenerate the desired acidic oligomers (Scheme S1). According to our attempts, for example in the case of tertiary amine as *N,N*-diisopropylethylamine (DIPEA), 3 equivalents of Amberlyst were necessary (therefore, double quantity for secondary amines). There were traces of ammonium left which were not removed with higher Amberlyst-15 loading. Amberlyst 15 was added in the diluted reaction mixture in dichloromethane. After 15 min stirring at 18 °C, it was filtered off and the homogeneous solution was concentrated under reduced pressure. The removal was confirmed by ^1H NMR spectroscopy with the vanishing of DIPEA ammonium signal (Figure S2).



Scheme S1 : Ion exchange between formed carboxylate ammonium and Amberlyst-15.

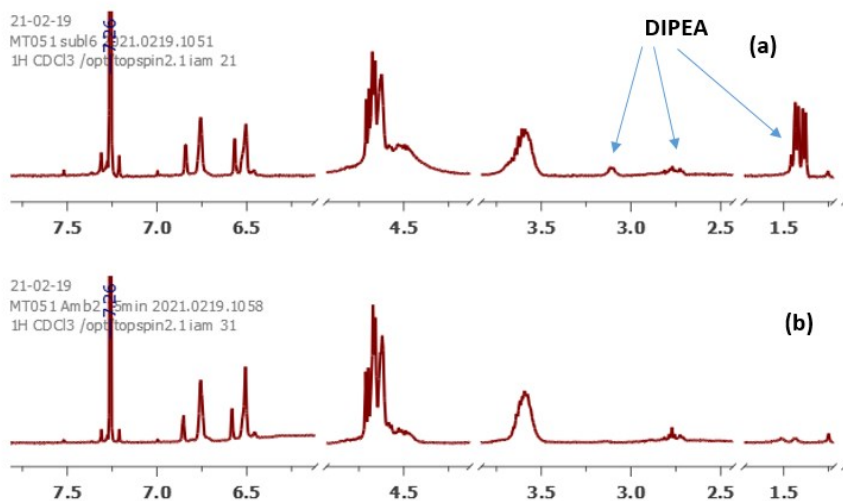


Figure S2: ^1H NMR spectra (in CDCl_3) of the crude of the reaction with DIPEA (5 mol%) (Entry 9 - Table 1) (a) before and (b) after filtration on Amberlyst 15.

Sublimation

Optimisation

The evolution of the MAF elimination was monitored by ^1H NMR. As the oligomers were not sublimated in our conditions and their quantities did not change, the integration of the vinylic CH of the oligomers was set to 1 to facilitate the interpretation. The unreacted MAF removal efficiency was determined with the formula :

$$\text{MAF removal efficiency (\%)} = \frac{\frac{\int_{6.8}^{6.9} CH(\text{crude})}{\int_{6.7}^{6.8} CH(\text{crude})} - \frac{\int_{6.8}^{6.9} CH(\text{SublX})}{\int_{6.7}^{6.8} CH(\text{SublX})}}{\frac{\int_{6.8}^{6.9} CH(\text{SublX})}{\int_{6.7}^{6.8} CH(\text{SublX})}} \times 100$$

The crude of the reaction with KOH was engaged (Entry 5 - Table 1 and Figure S3, Crude). The sublimation was attempted firstly with the round bottom apparatus 1 at 100 °C for 30 min (Figure S3, Sublimation 1). The MAF was removed quite efficiently, the integration of the vinylic CH of MAF dropped from 1.16 to 0.26, corresponding to 78% removal efficiency. The flat bottom sublimation apparatus 2 was then used. Slightly higher removal efficiency was observed at 60 °C (Figure S3, Sublimation 2) . Higher temperature (100°C) did not improve the MAF removal (Figure S3, Sublimation 3). The optimal condition consists in the use of the apparatus 2 at 60°C. We believe that the flat bottom allows to have thinner and more regular layer of crude material on the glassware, comparing to the round bottom one, making the MAF elimination more efficient. Longer sublimation time (1-2 h) allowed to remove all traces of MAF.

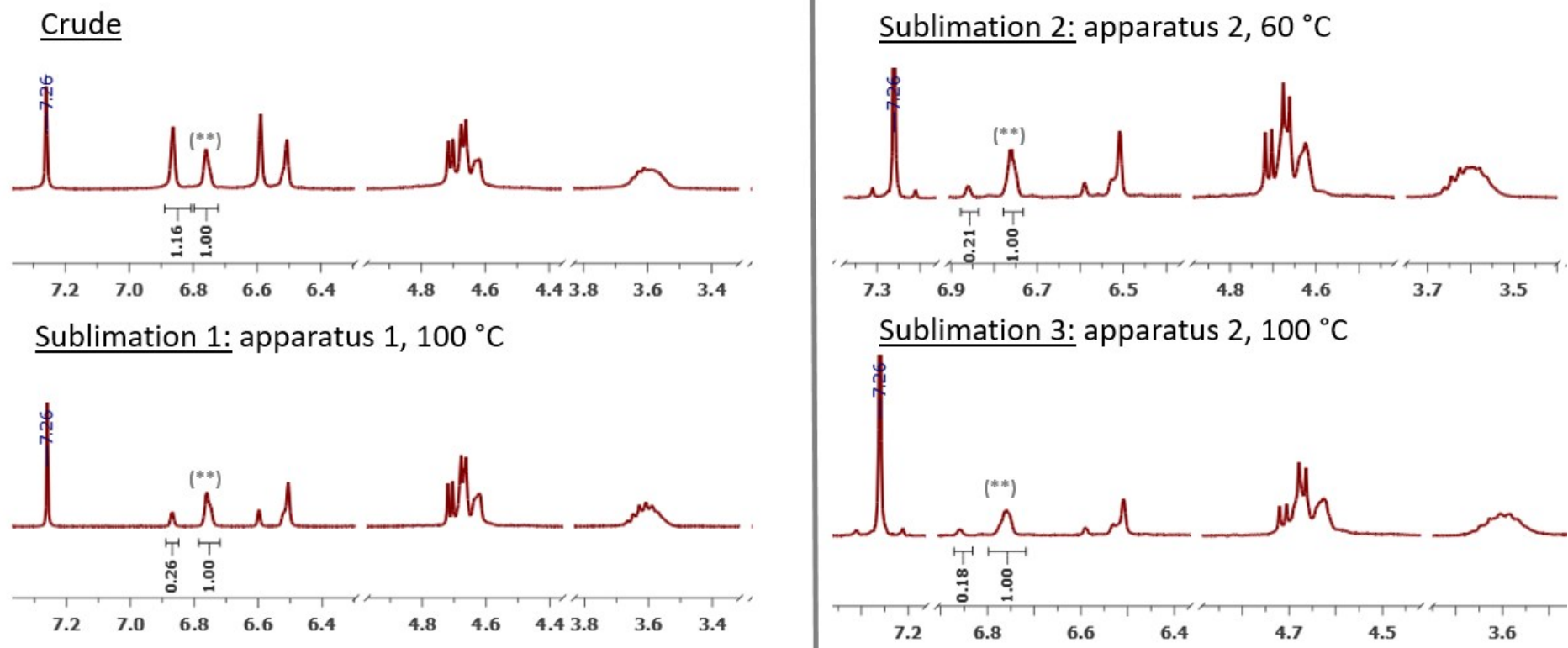


Figure S3 : ^1H NMR spectra (in CDCl_3) of different sublimation attempts ; (**): unchanged integral of $\text{CH}_{\text{ethylenic-oligomers}}$

Procedure

After being cooled down to room temperature, the reaction mixture was diluted in dichloromethane and transferred into the bottom of the sublimation apparatus. The solution was stirred and heated at 40 °C under air flow to remove the solvent in a mild and rapid way. Then, the apparatus was closed and put under reduced pressure to remove all traces of solvent and water. The temperature of the oil bath (60 °C) and the condenser (15 °C) were set up. The experience proceeded then for 1 h to 2 h and monitored by NMR spectroscopy.

Characterisation of MAF

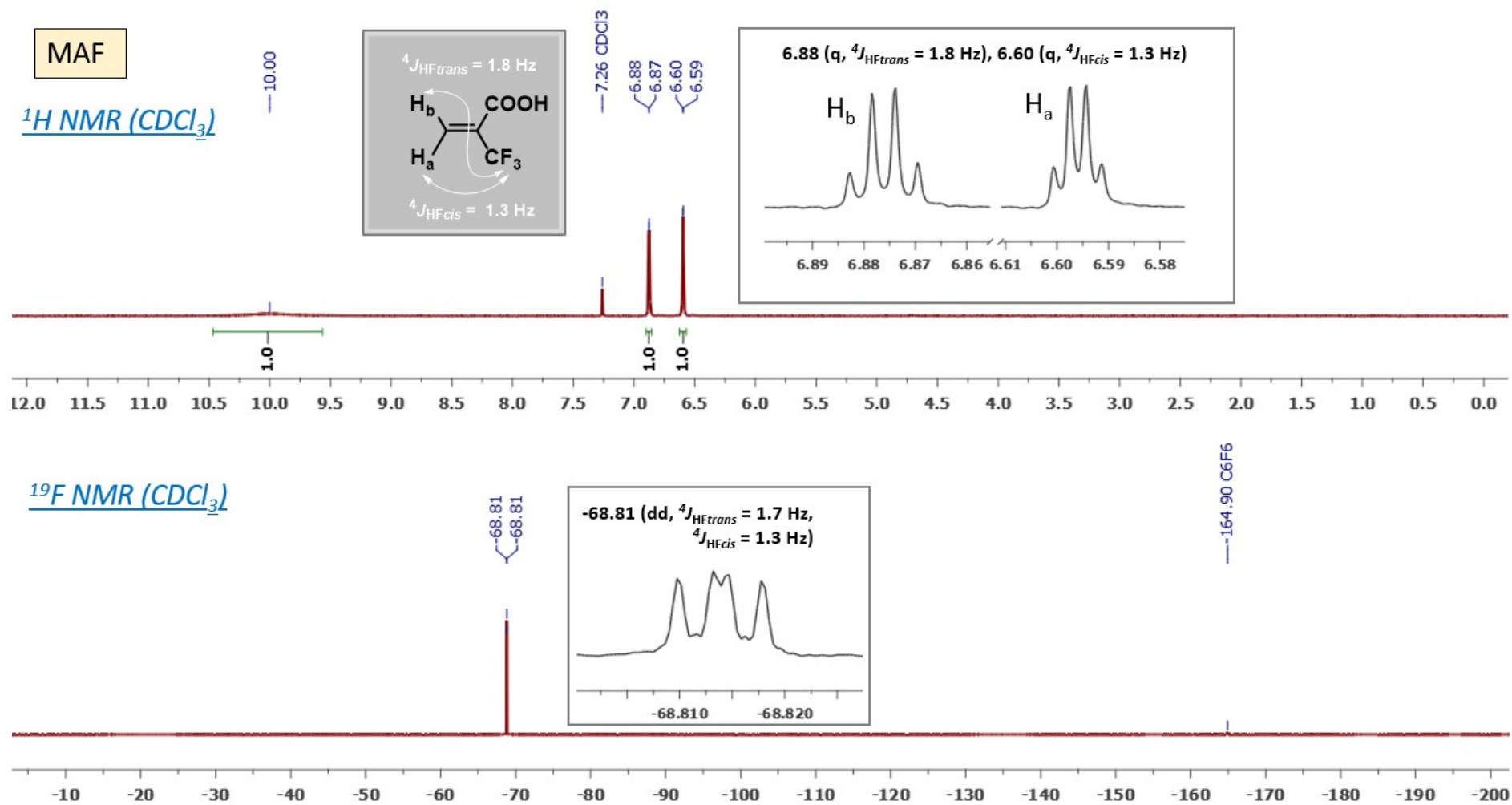


Figure S4 : ^1H (top) and ^{19}F (bottom) NMR spectra (in CDCl_3) of MAF.

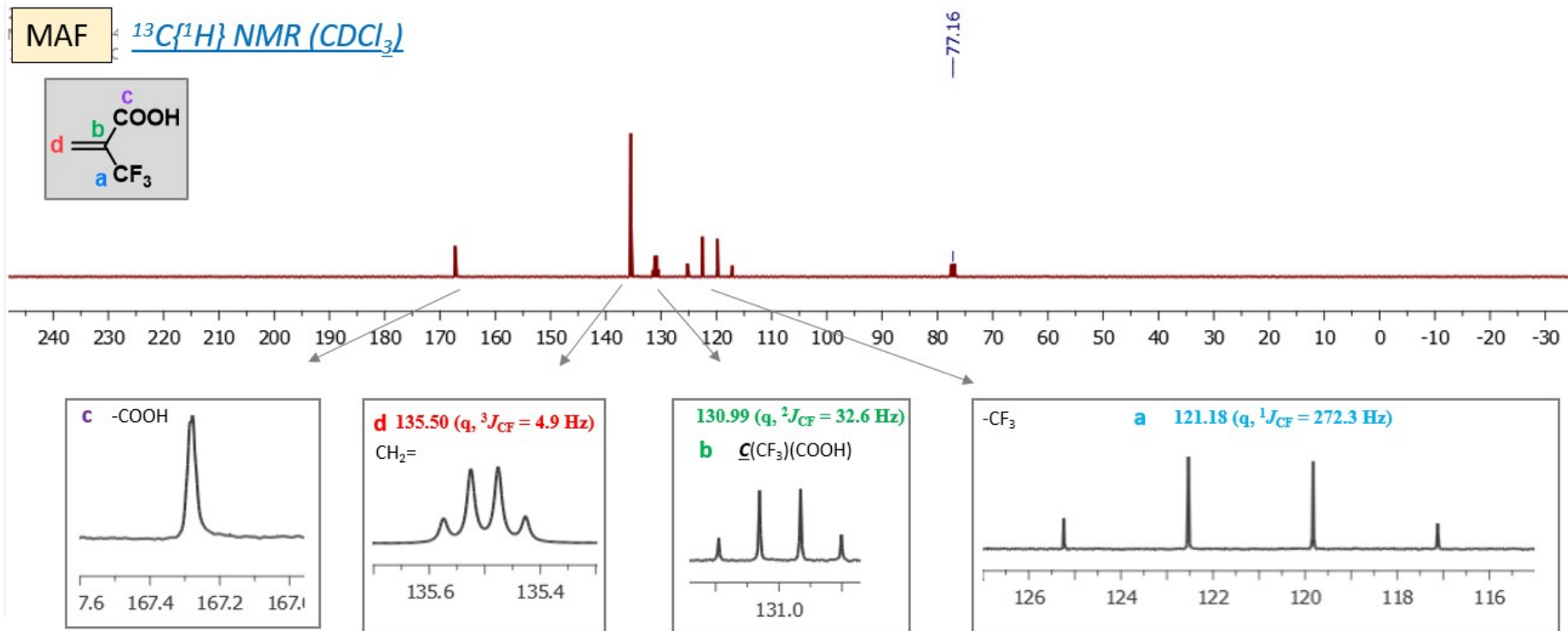
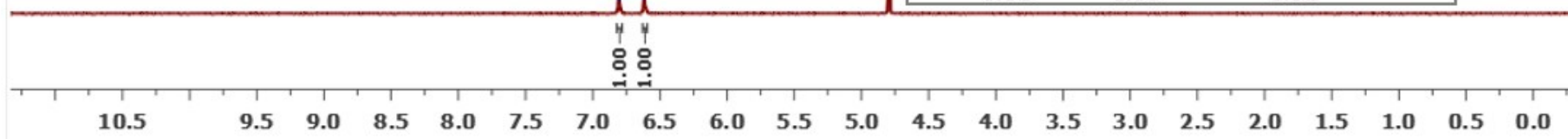
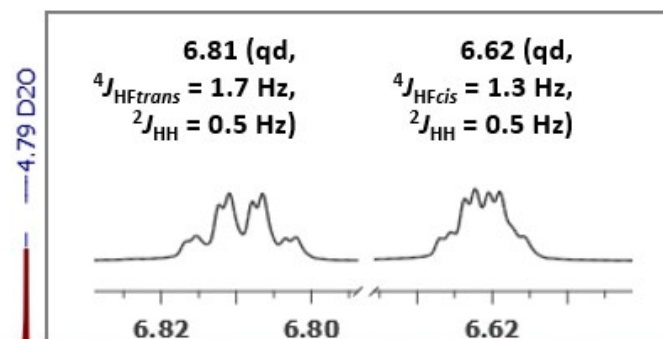
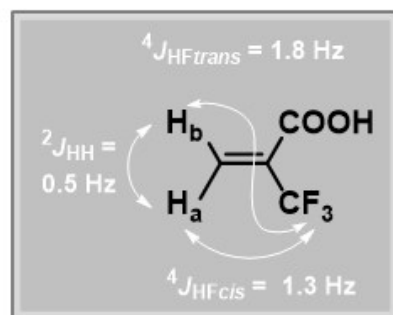


Figure S5: $^{13}\text{C}\{^1\text{H}\}$ NMR spectrum (in CDCl_3) of MAF

MAF

^1H NMR (D_2O)



^{19}F NMR (D_2O)

-67.36
-67.36

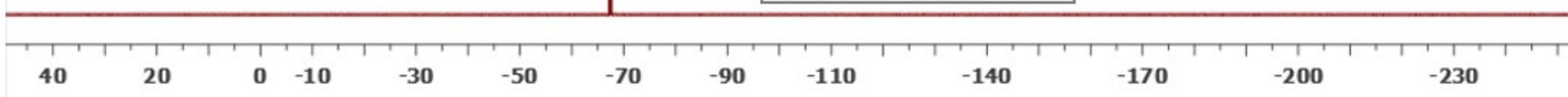
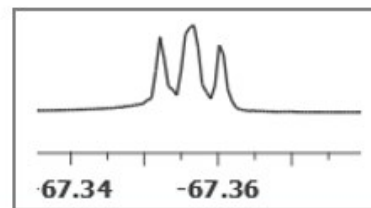


Figure S6 : ^1H and ^{19}F NMR spectra (in D_2O) of MAF

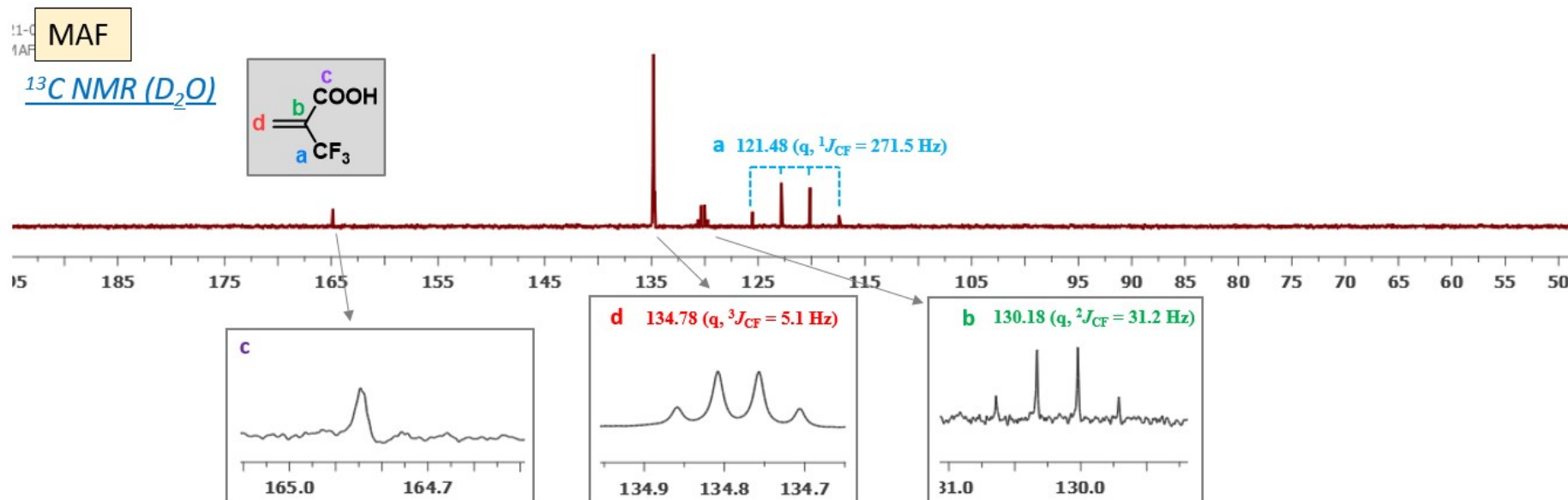


Figure S7 : $^{13}\text{C}\{^1\text{H}\}$ NMR spectrum (in D_2O) of MAF

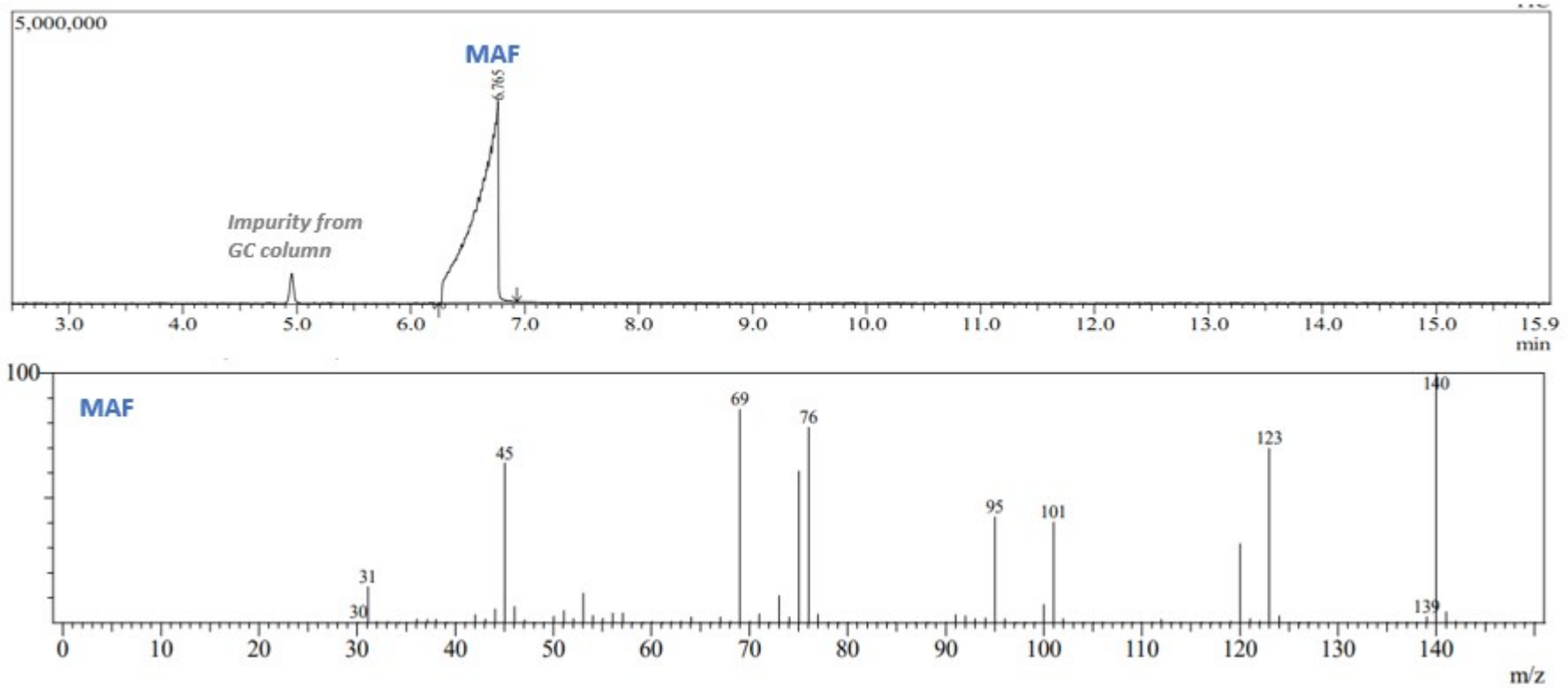


Figure S8 : GC (top)/MS (bottom) spectra of MAF, $m/z = 140$ (base peak, MAF), $m/z = 45$ (CHO_2^*), 69 (CF_3^*), 95 ($\text{C}_3\text{H}_2\text{F}_3^*$), 123 ($\text{C}_4\text{H}_2\text{F}_3\text{O}^*$)

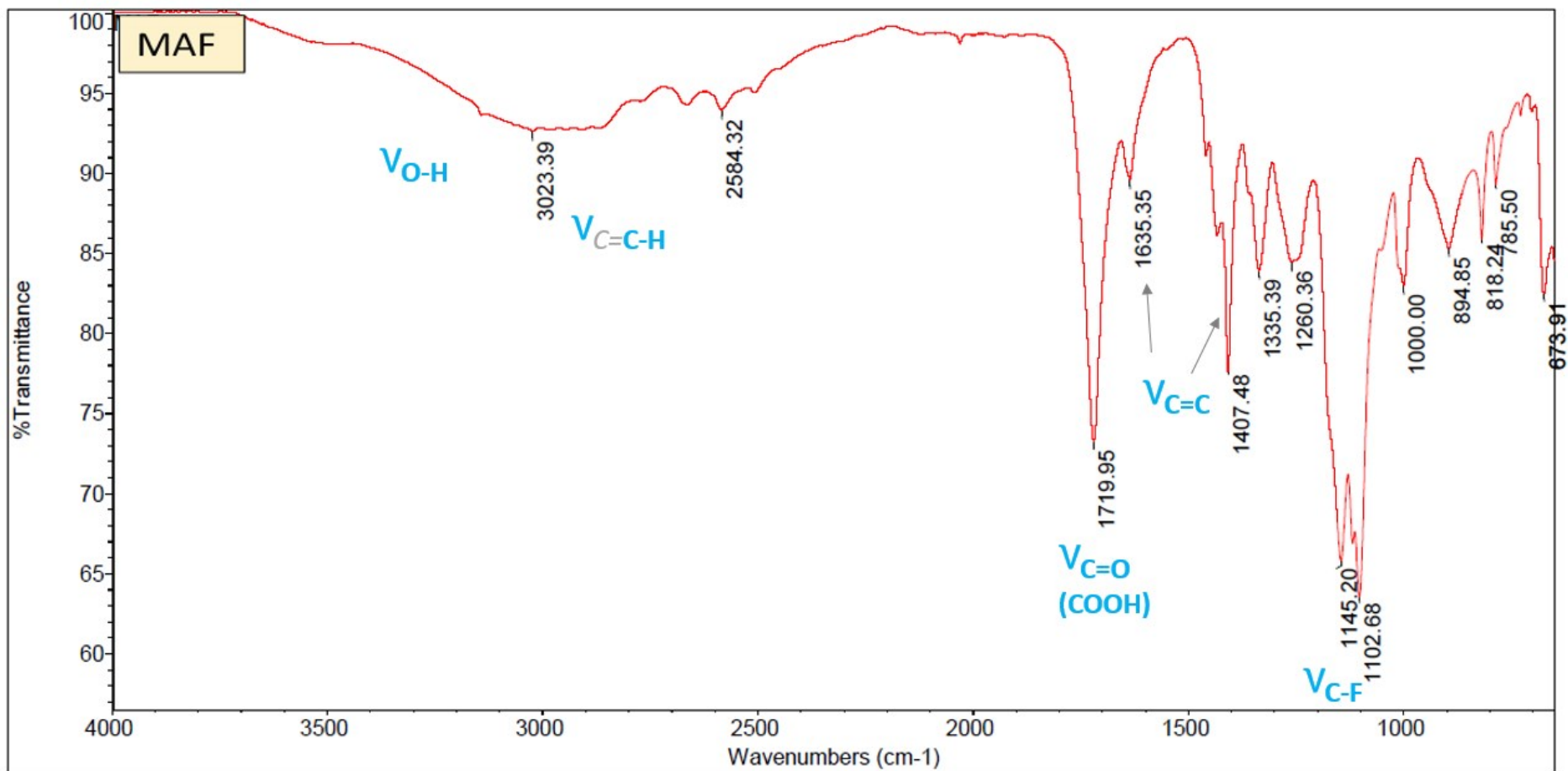


Figure S9 : ATR-IR spectrum of MAF

Characterisation of diMAF and triMAF

Characterisation of diMAF from MAF/diMAF mixture (Entry 1 – Table 1)

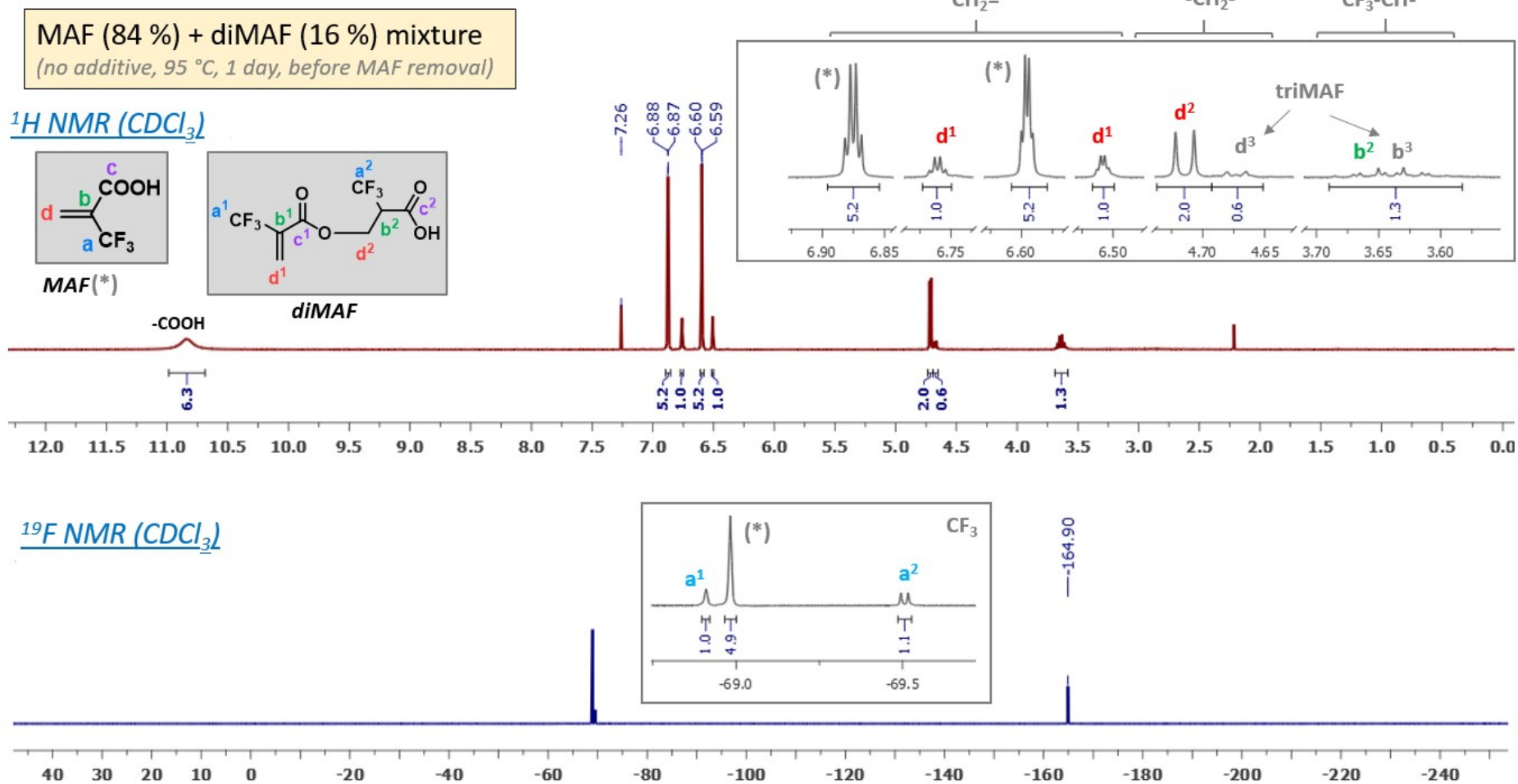
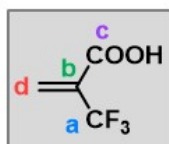


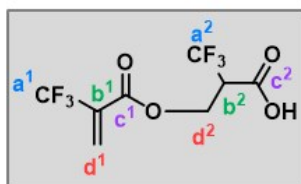
Figure S10: ¹H and ¹⁹F NMR spectra (in CDCl₃) of the mixture of MAF and diMAF, obtained without additive (Entry 1 – Table 1), the starred signals are assigned to unreacted MAF

MAF (84 %) + diMAF (16 %) mixture
 (no additive, 95 °C, 1 day, before MAF removal)

$^{13}\text{C}\{^1\text{H}\}$ APT NMR (CDCl_3)



MAF(*)



diMAF

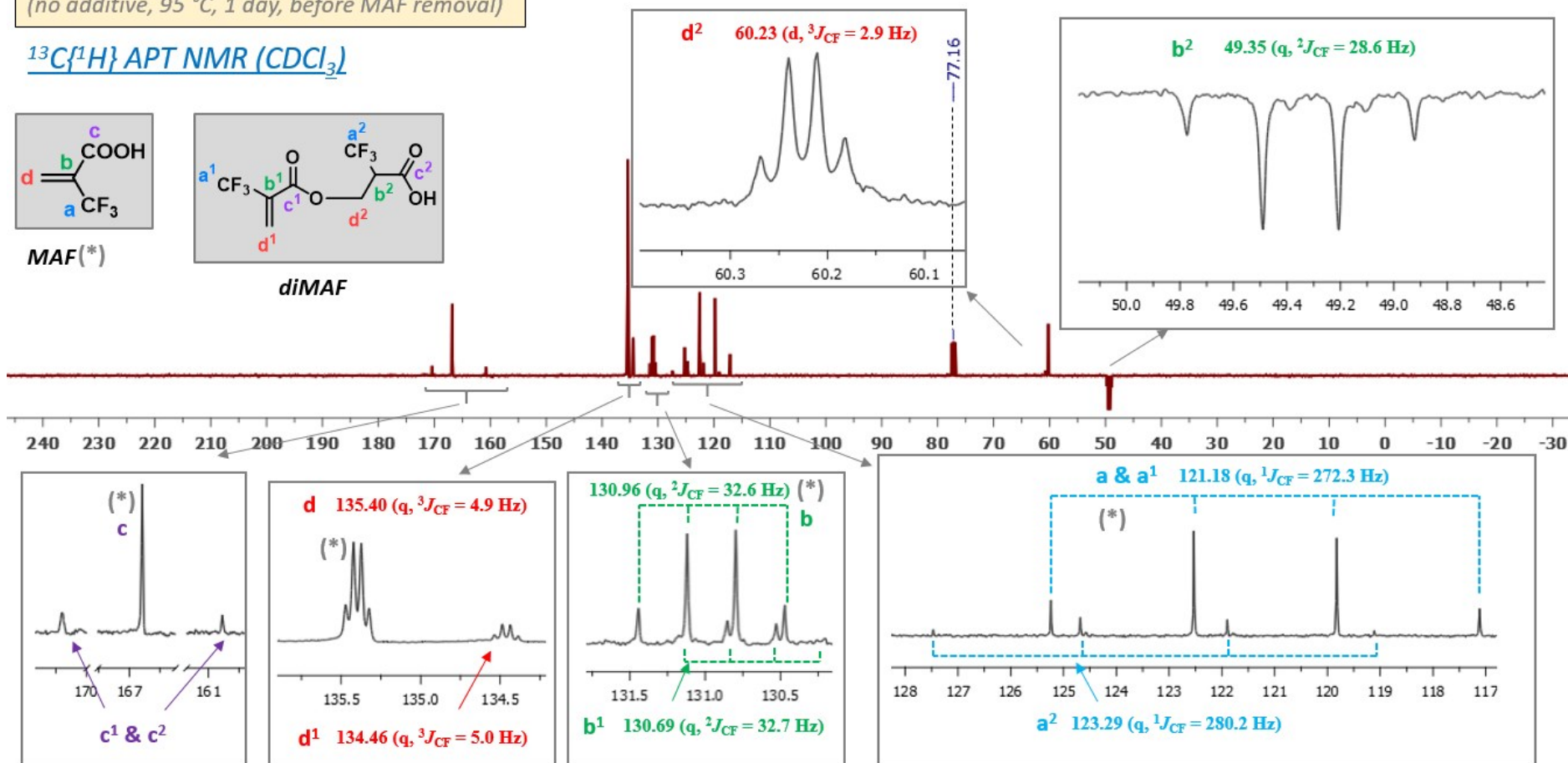
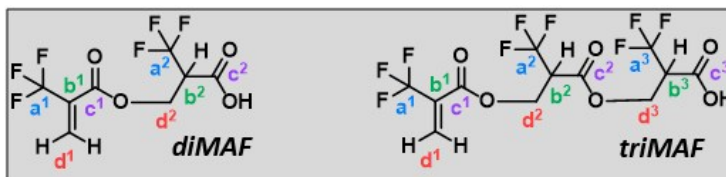


Figure S11 : $^{13}\text{C}\{^1\text{H}\}$ -APT NMR spectrum (in CDCl_3) of the mixture of MAF and diMAF, obtained without additive (Entry 1 – Table 1), the starred signals are assigned to unreacted MAF

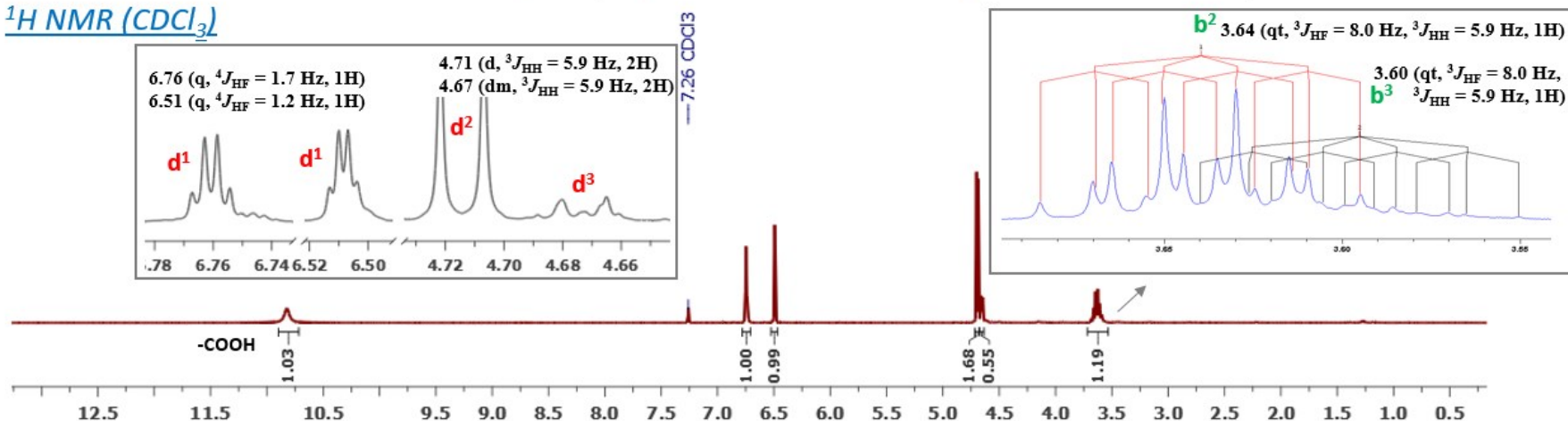
Characterisation of triMAF from diMAF/triMAF mixture (Entry 1 – Table 1)

DiMAF (67 %) + triMAF (33 %)

(no additive, 95 °C, 1 day, after MAF removal)



^1H NMR (CDCl_3)



$^1\text{H}\{^{19}\text{F}\}$ NMR (CDCl_3)

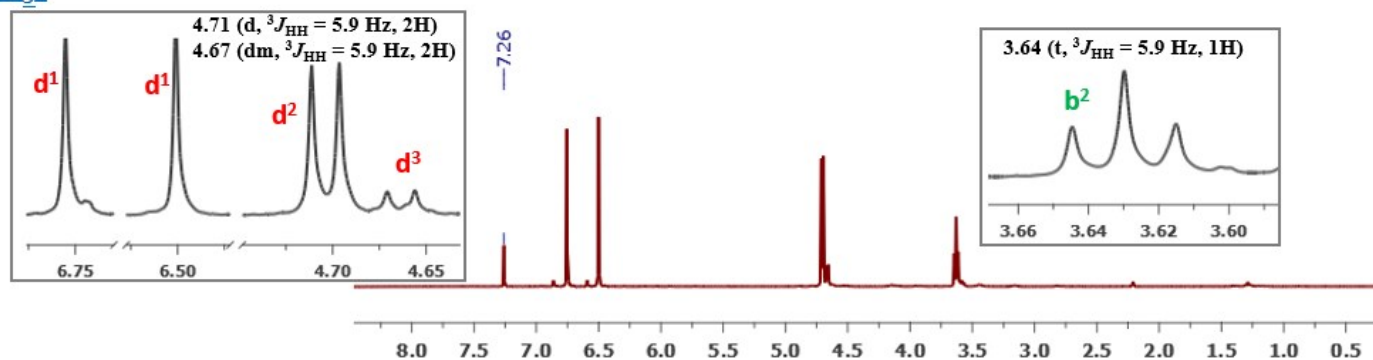


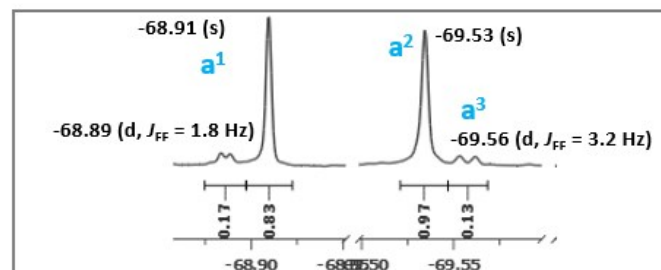
Figure S12 : ^1H (top) and $^1\text{H}\{^{19}\text{F}\}$ (bottom) NMR spectrum (in CDCl_3) of diMAF/triMAF mixture, obtained without additive (Entry 1 – Table 1).

DiMAF (67 %) + triMAF (33 %)

(no additive, 95 °C, 1 day, after MAF removal)

^{19}F $\{^1\text{H}\}$ NMR (CDCl_3)

^{19}F $\{^1\text{H}\}$ $\{^{13}\text{C}\}$ NMR (CDCl_3)



^{19}F NMR (CDCl_3)

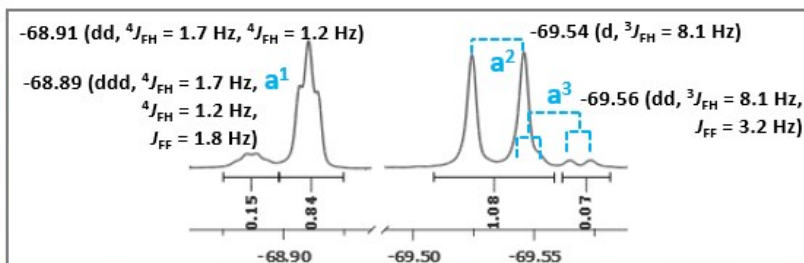
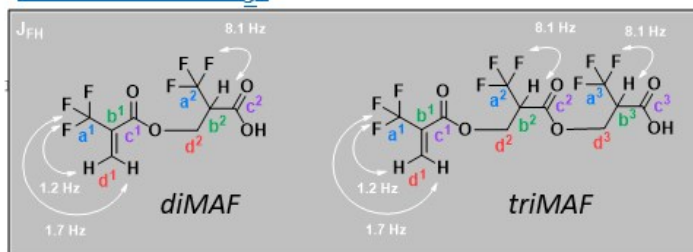


Figure S13 : ^{19}F $\{^1\text{H}\}$, ^{19}F $\{^1\text{H}\}$ $\{^{13}\text{C}\}$ (top –same profile) and ^{19}F (bottom) NMR spectra (in CDCl_3) of diMAF/triMAF mixture, obtained without additive (Entry 1 – Table 1).

DiMAF (67 %) + triMAF (33 %)
 (no additive, 95 °C, 1 day, after MAF removal)

$^{13}\text{C}\{^1\text{H}\}$ APT NMR (CDCl_3)

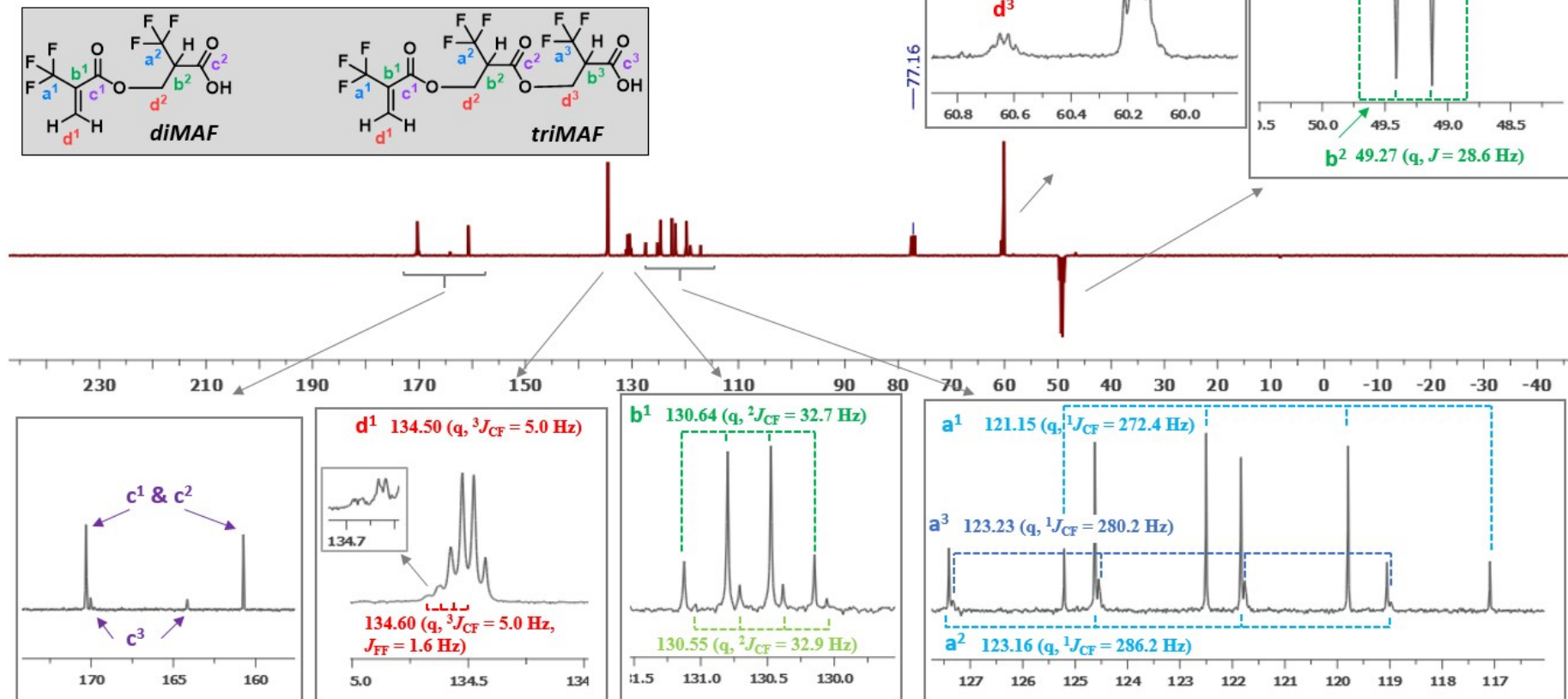


Figure S14 : $^{13}\text{C}\{^1\text{H}\}$ -APT NMR spectrum (in CDCl_3) of diMAF/triMAF mixture, obtained without additive (Entry 1 – Table 1), and expansions of the signals.

DiMAF + triMAF (no additive, 95 °C, 1 d, after MAF removal)

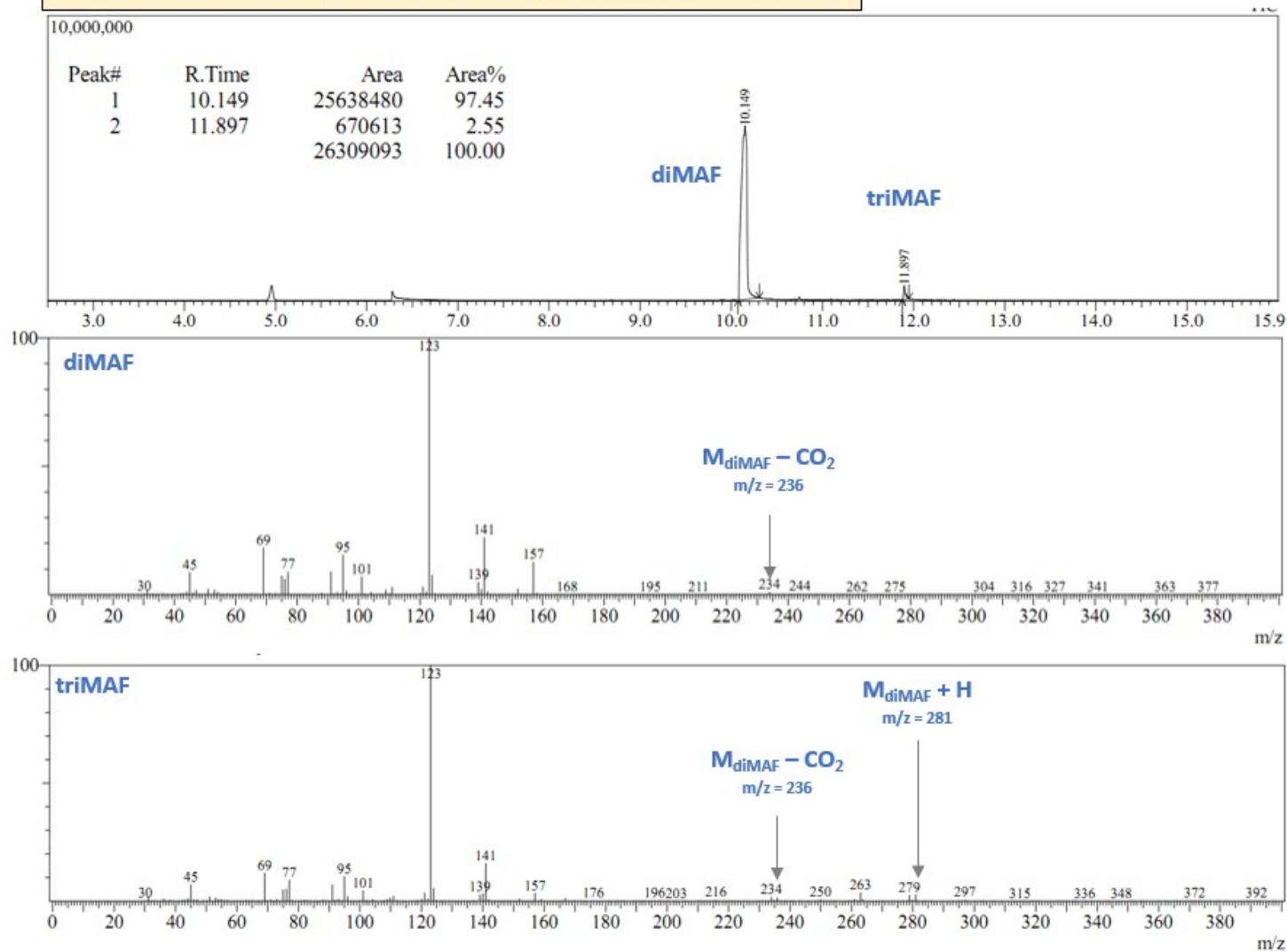


Figure S15 : GC (top)/MS (middle and bottom) spectra of diMAF and triMAF, obtained without additive (Entry 1 – Table 1).

Characterisation of oligoMAF

OligoMAF obtained without additive, 105 °C, 63h and after MAF removal (Entry 2 – Table 1)

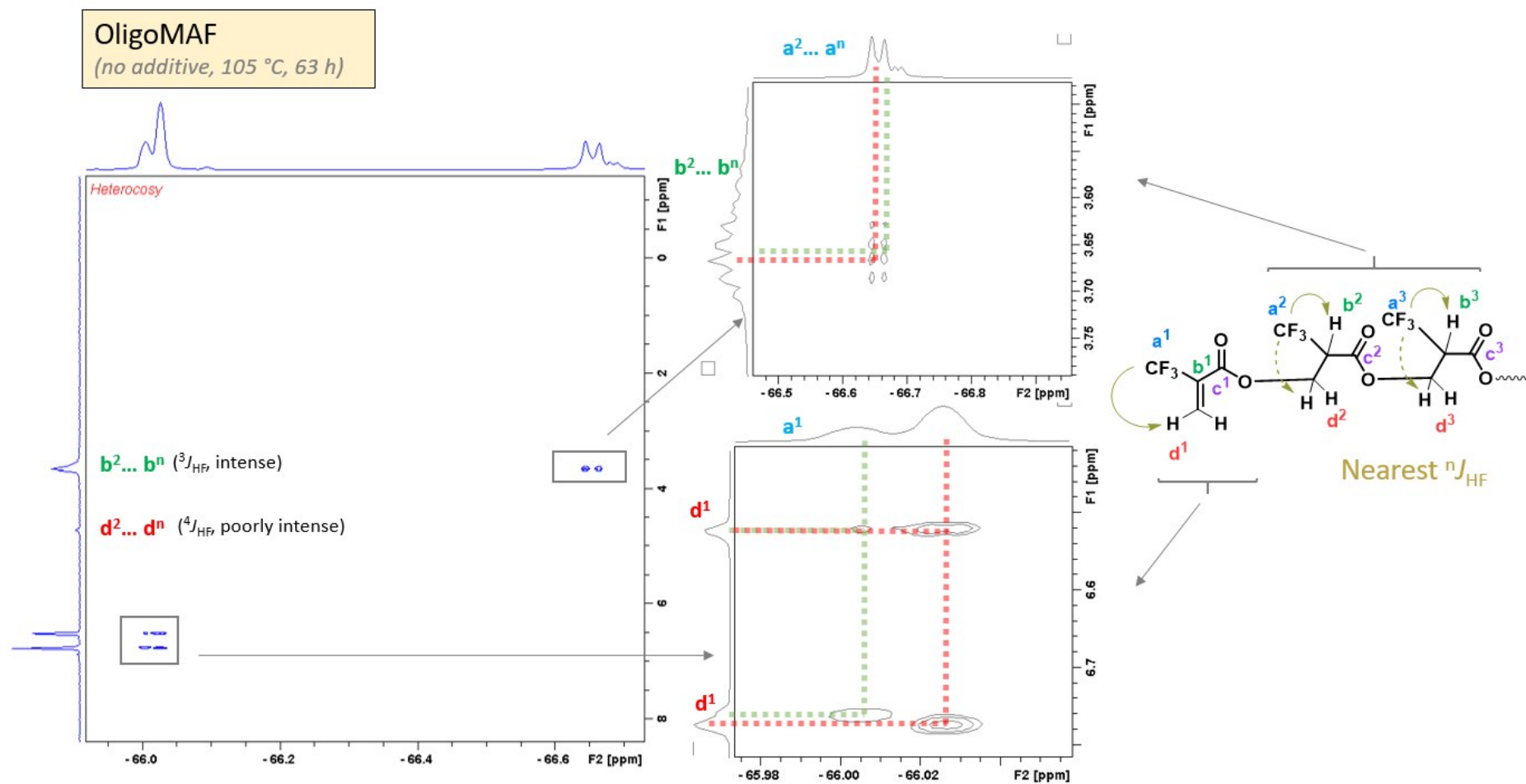


Figure S16 : HeteroCOSY ^1H - ^{19}F spectrum (in CDCl_3) of oligoMAF and its expansions. The one-dimensional spectra are plotted at the top (^{19}F) and left (^1H) of the 2D plots.

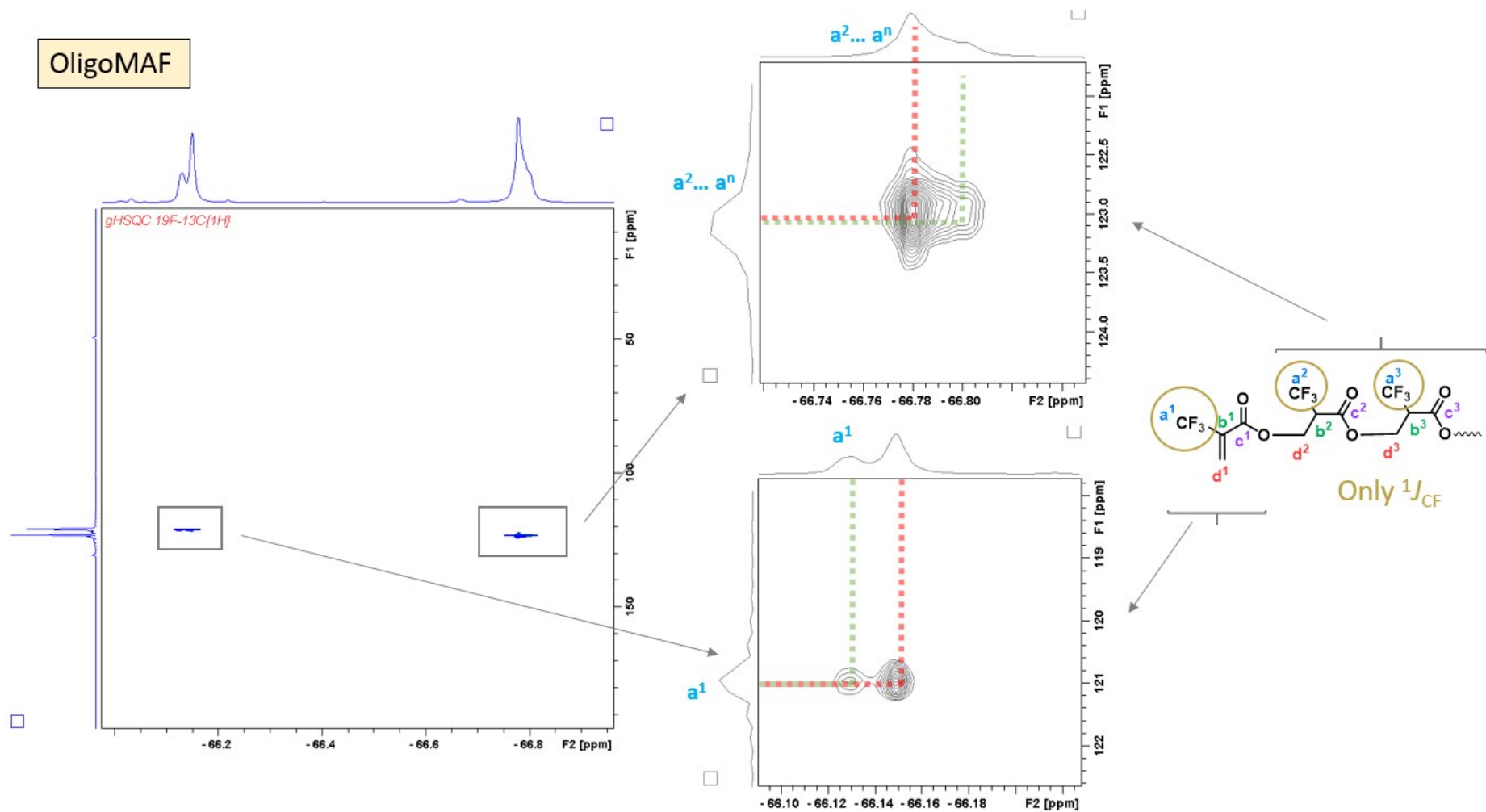


Figure S17 : gHSQC spectrum (in CDCl₃) of oligoMAF and its expansions. The one-dimensional spectra are plotted at the top (¹⁹F{¹H}) and left (¹³C{¹H}-APT) of the 2D plots. Only signals involved $^1J_{CF}$ are displayed.

Further characterisation of the structure of synthesised oligoMAF (Entry 2-Table 1) was performed *via* MALDI-TOF spectroscopy. The positive reflectron spectrum (Figure S18) exhibits one signal series with unsymmetric Gaussian shape distribution. This series is assigned to sodium adducts [oligoMAF + Na]⁺, ranging between $m/z = 443$ (DP₃) and $m/z = 1703$ (DP₁₂), separated by repeated 140 units of MAF (CH₂CHCF₃COO) and centered on pentaMAF $m/z = 723$. The expansion between 550 m/z and 890 m/z , corresponding to DP₄₋₆, is supplied in inset. M_n and M_w values are 711 and 770, respectively, leading to a dispersity of 1.1. In addition, the experimental masses of oligoMAF ($y = 3, 4, 5$ and 6) are consistent with the theoretical ones (Table S1). MS-MS analysis of 723 m/z fragment ($y = 5$, Figure S19) shows sodium adducts (masses in red) and the complementary fragments (masses in black), resulted from the cleavage of (CF₃)C-COO, (O)CO-CH₂ and C(O)-O bonds.

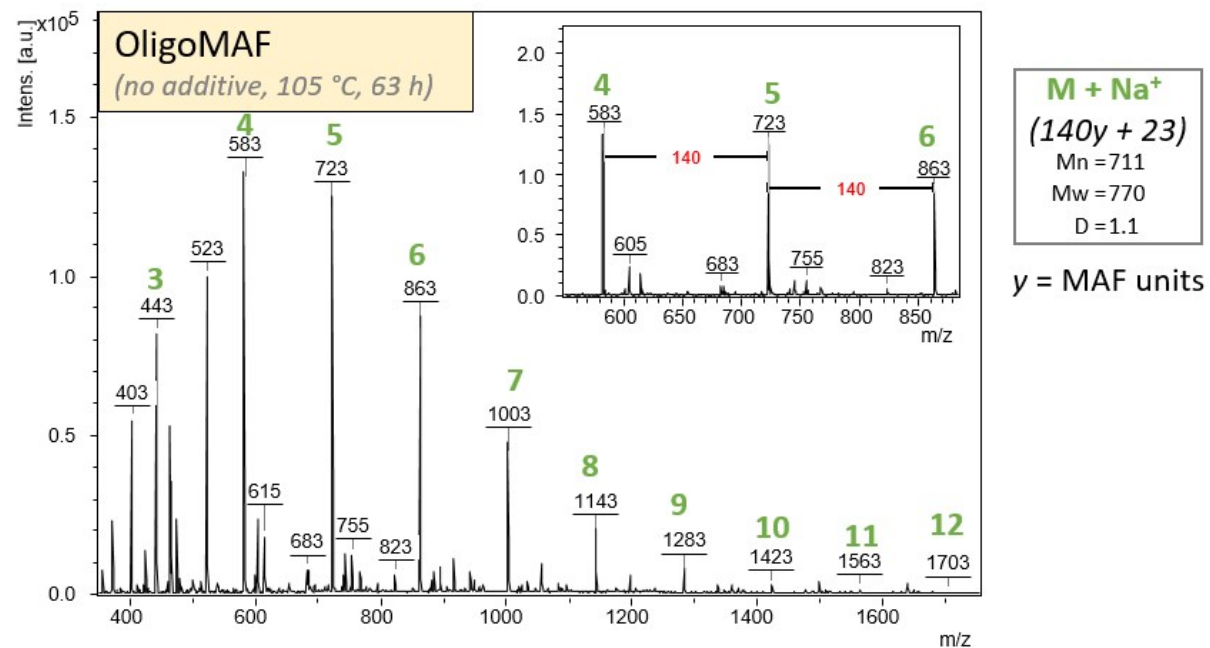


Figure S18 : MALDI-TOF mass positive reflectron spectrum with expansion from 550 and 890 m/z with NaI as cationizing agent and *trans*-2-[3-(4-*tert*butylphenyl)-2-methylprop-2-enylidene]malononitrile (DCTB) as the matrix (Entry 2-Table 1). $\overline{DP}_n = 5$ was determined with MALDI-TOF.

Table S1 : Mass attribution of MALDI-TOF signals of oligoMAF

Experimental mass (m/z) ($M_n + Na$) ⁺	Theoretical mass (m/z) ($M_n + Na$) ⁺	Formula (M_n)
443.08	443.02	CH ₂ =C(CF ₃)COO-[CH ₂ CH(CF ₃)COO]-CH ₂ CH(CF ₃)COOH
583.09	583.02	CH ₂ =C(CF ₃)COO-[CH ₂ CH(CF ₃)COO] ₂ -CH ₂ CH(CF ₃)COOH
723.12	523.03	CH ₂ =C(CF ₃)COO-[CH ₂ CH(CF ₃)COO] ₃ -CH ₂ CH(CF ₃)COOH
863.14	863.04	CH ₂ =C(CF ₃)COO-[CH ₂ CH(CF ₃)COO] ₄ -CH ₂ CH(CF ₃)COOH

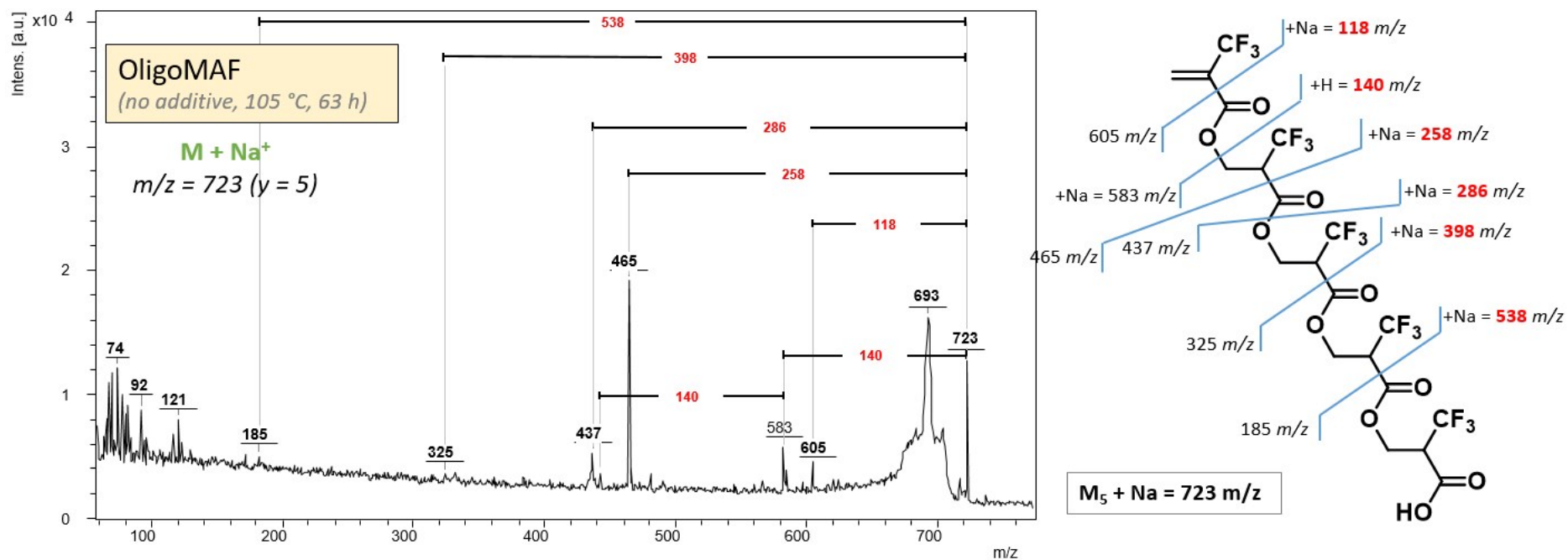


Figure S19 : MS-MS fragmentation analysis of 723 m/z (pentaMAF)

OligoMAF obtained from DIPEA (5 mol%) (Entry 9-Table 1)

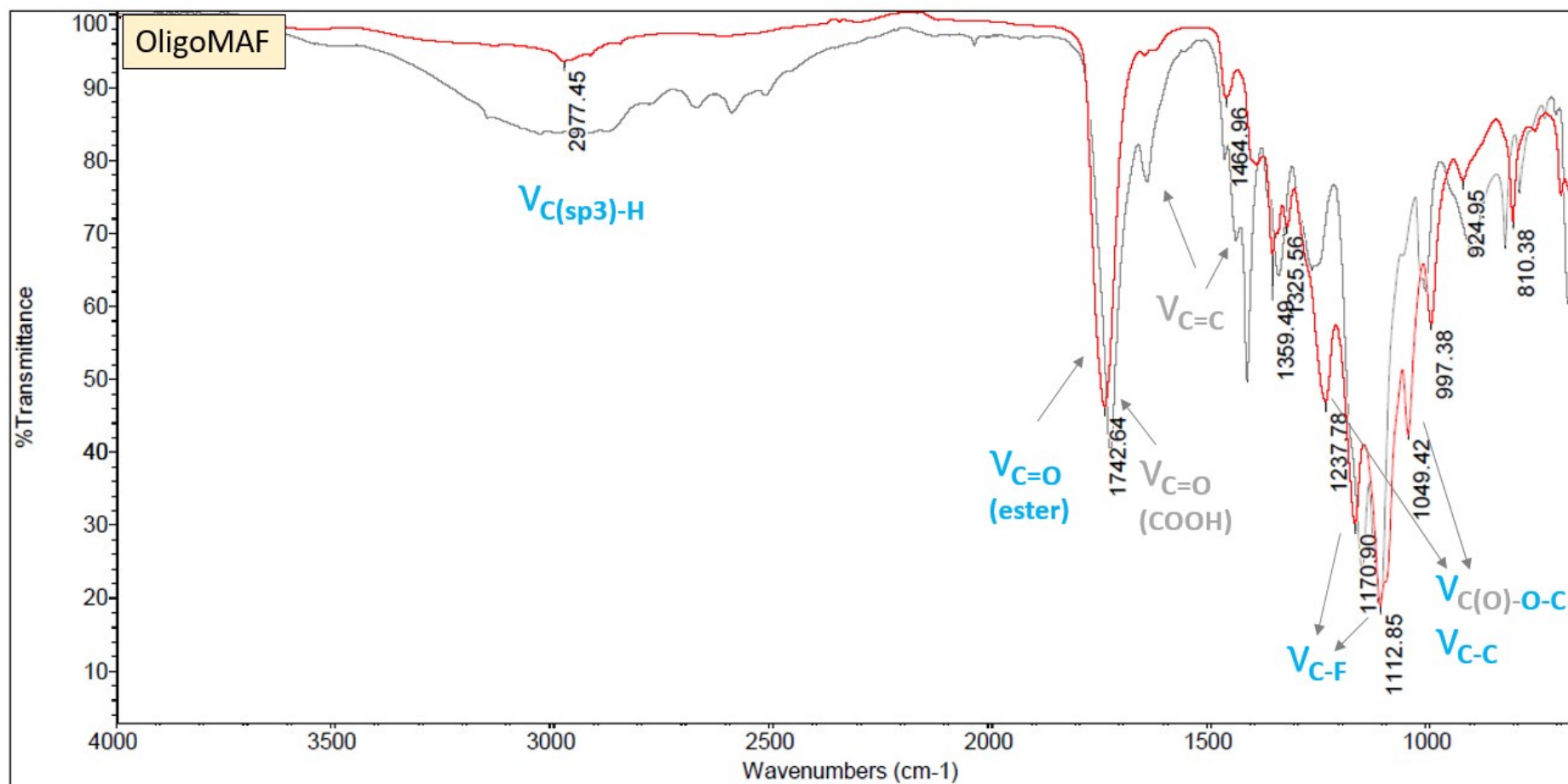


Figure S20 : IR spectra of MAF (grey) and oligoMAF (red - obtained with DIPEA 5 mol%) (Entry 9-Table 1).

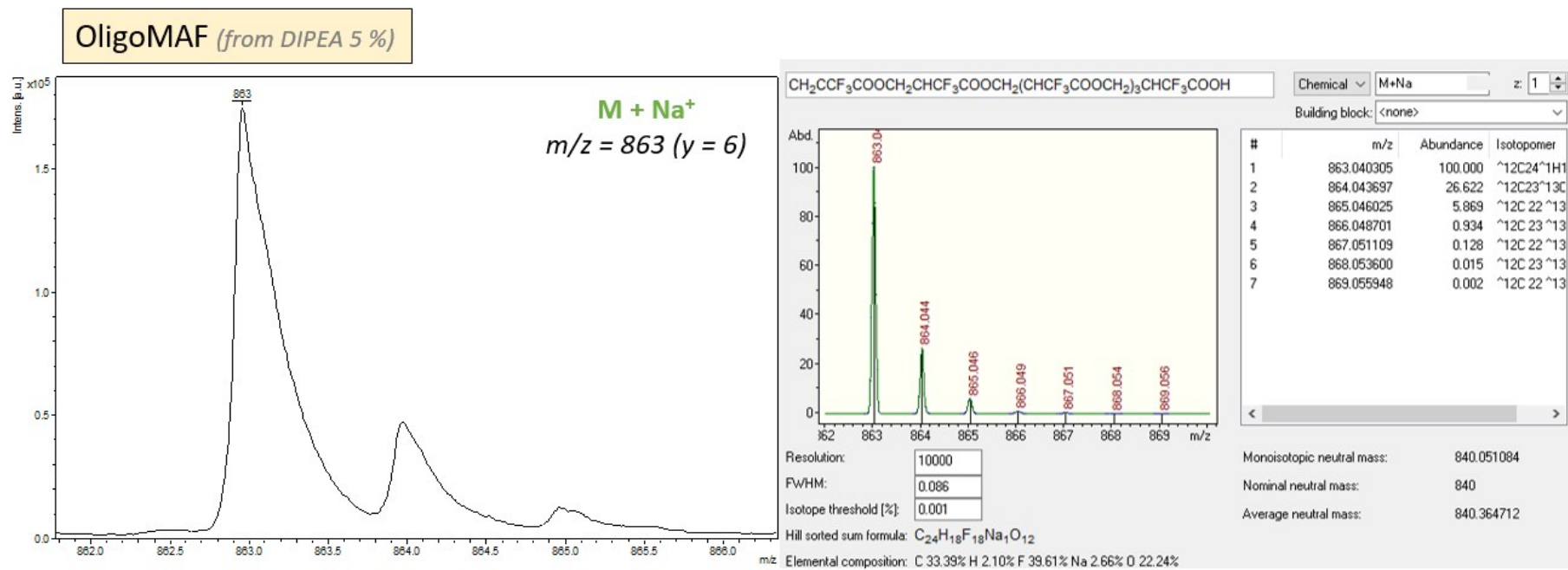


Figure S21: Isotopic distribution corresponding to signal m/z = 863 (hexaMAF) of MALDI-TOF (Entry 9-Table 1)

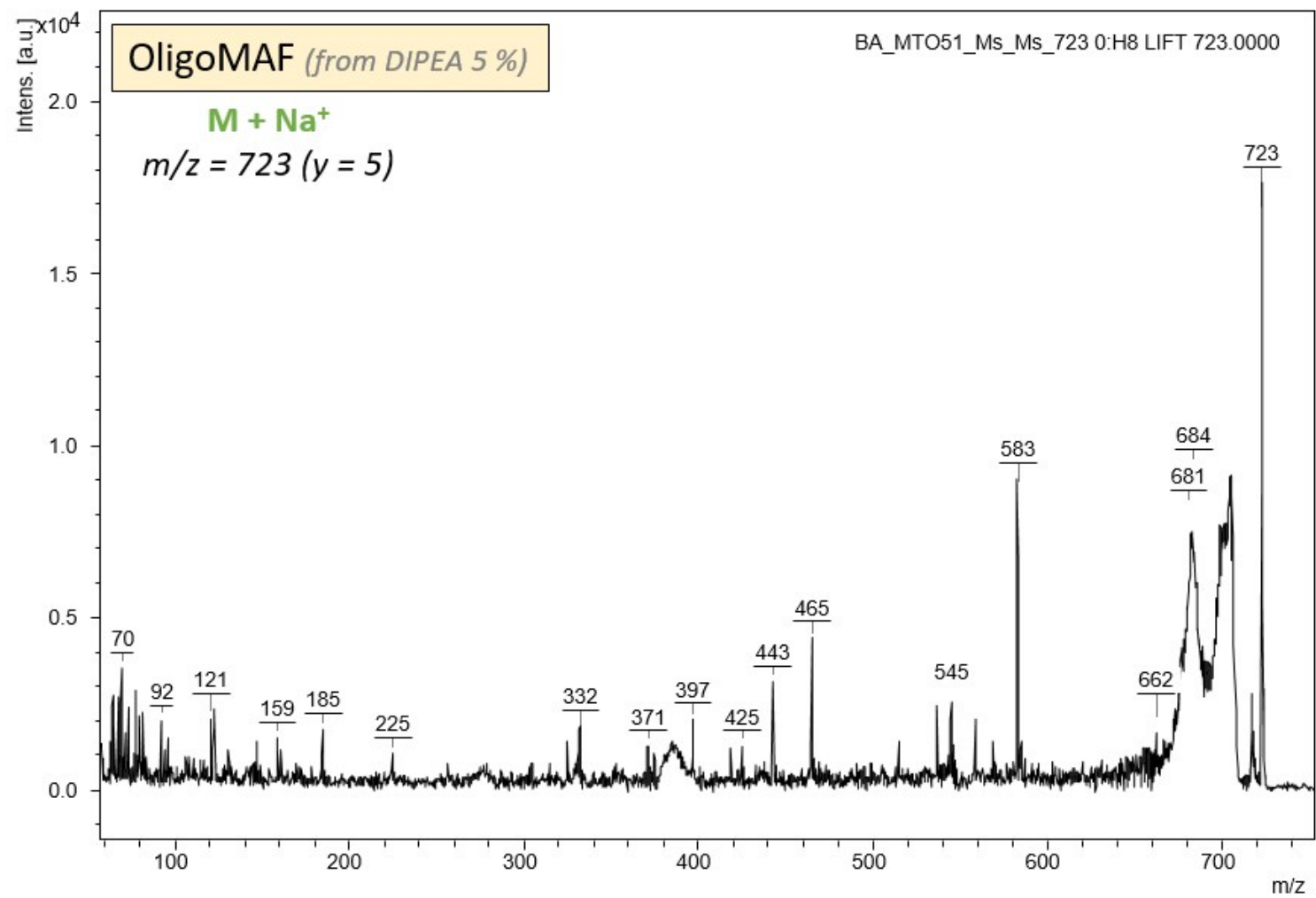


Figure S22 : MS-MS fragmentation analysis of 723 m/z

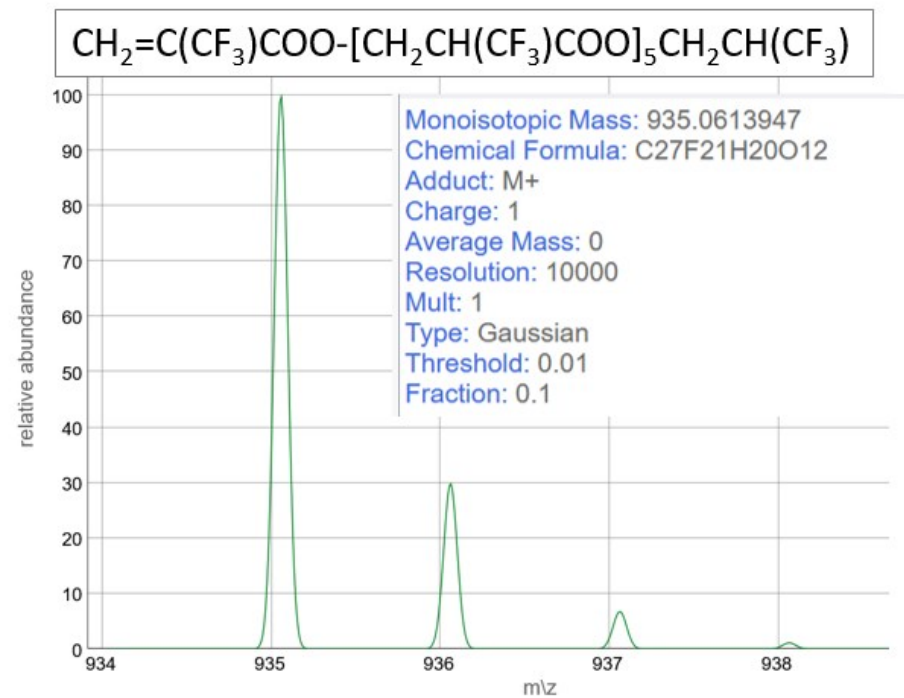
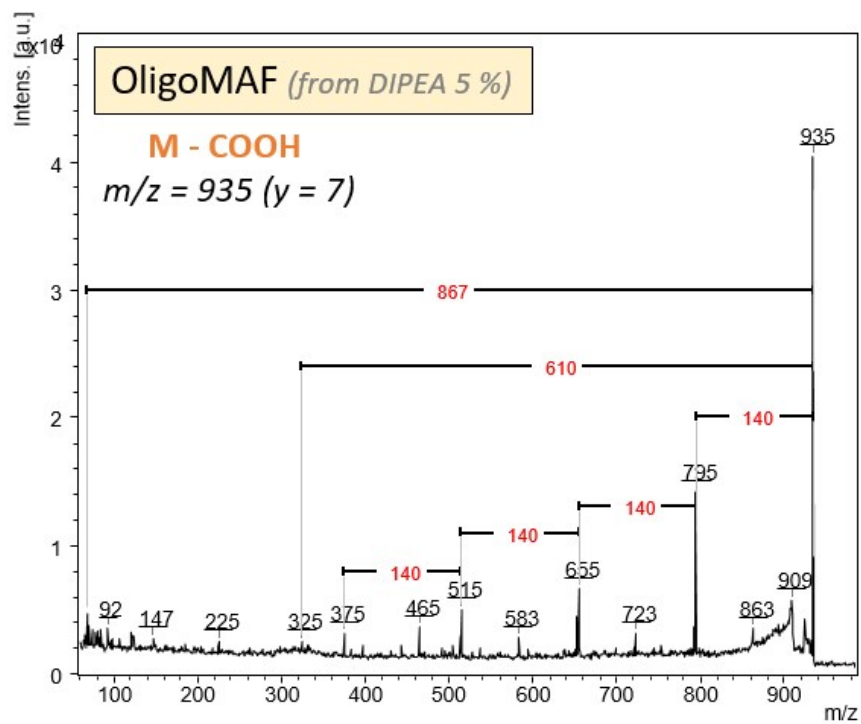
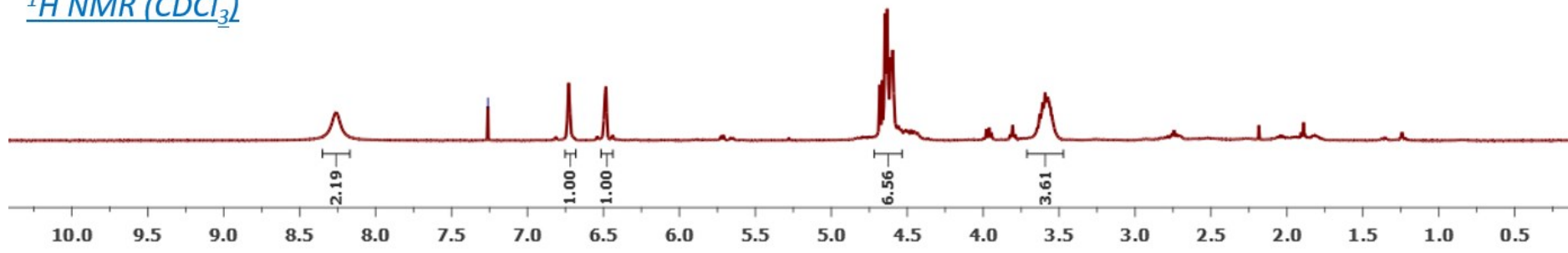


Figure S23 : MS-MS fragmentation analysis (left) and isotopic distribution (right) corresponding to signal 935 m/z = 863 (heptaMAF) of MALDI-TOF.

OligoMAF (DIPEA 5%)

—7.26

^1H NMR (CDCl_3)



^{19}F NMR (CDCl_3)

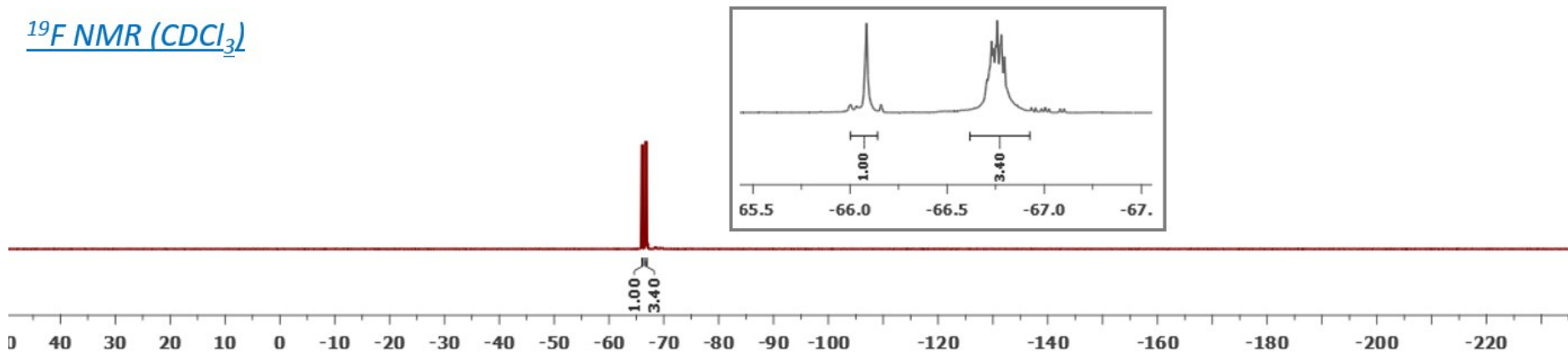


Figure S24 : ^1H (top) and ^{19}F (bottom) NMR spectra (in CDCl_3) of oligoMAF obtained by using DIPEA (5%) (Entry 9 – Table 1). $DP_n = 4.4$ and 4.6 were determined with ^1H and ^{19}F NMR, respectively.

Organic ammonium salt generated from MAF and 2,2,6,6-tetramethylpiperidine

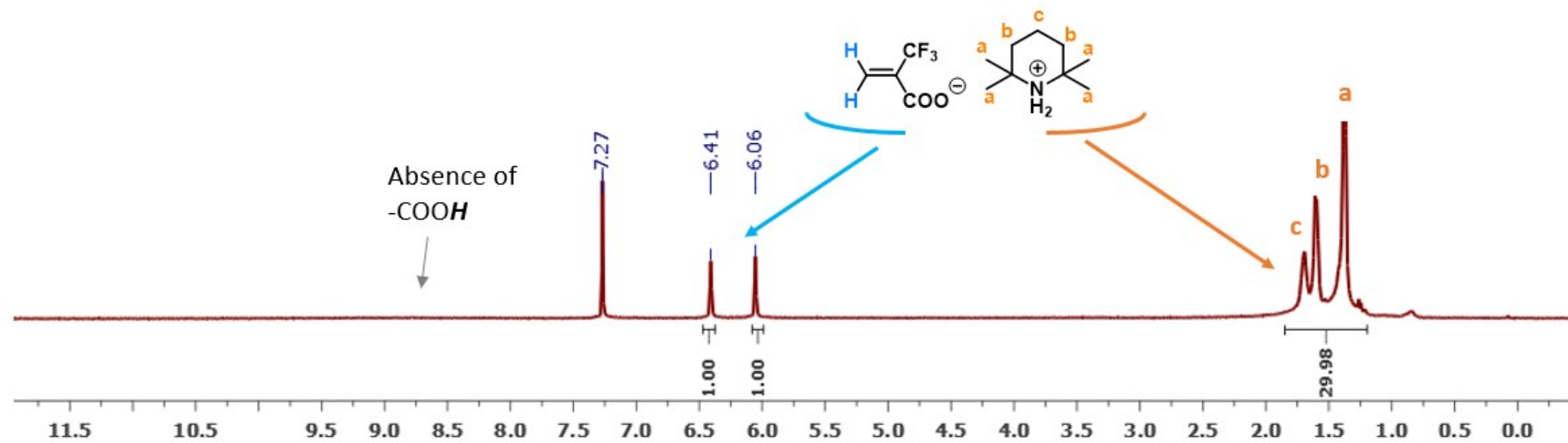


Figure S25 : ^1H NMR spectrum (in CDCl_3) of the organic ammonium salt generated from MAF and 2,2,6,6-tetramethylpiperidine

OligoMAF obtained with PPh_3 (5 mol% at 60 °C) (Entry 15 – Table 1)

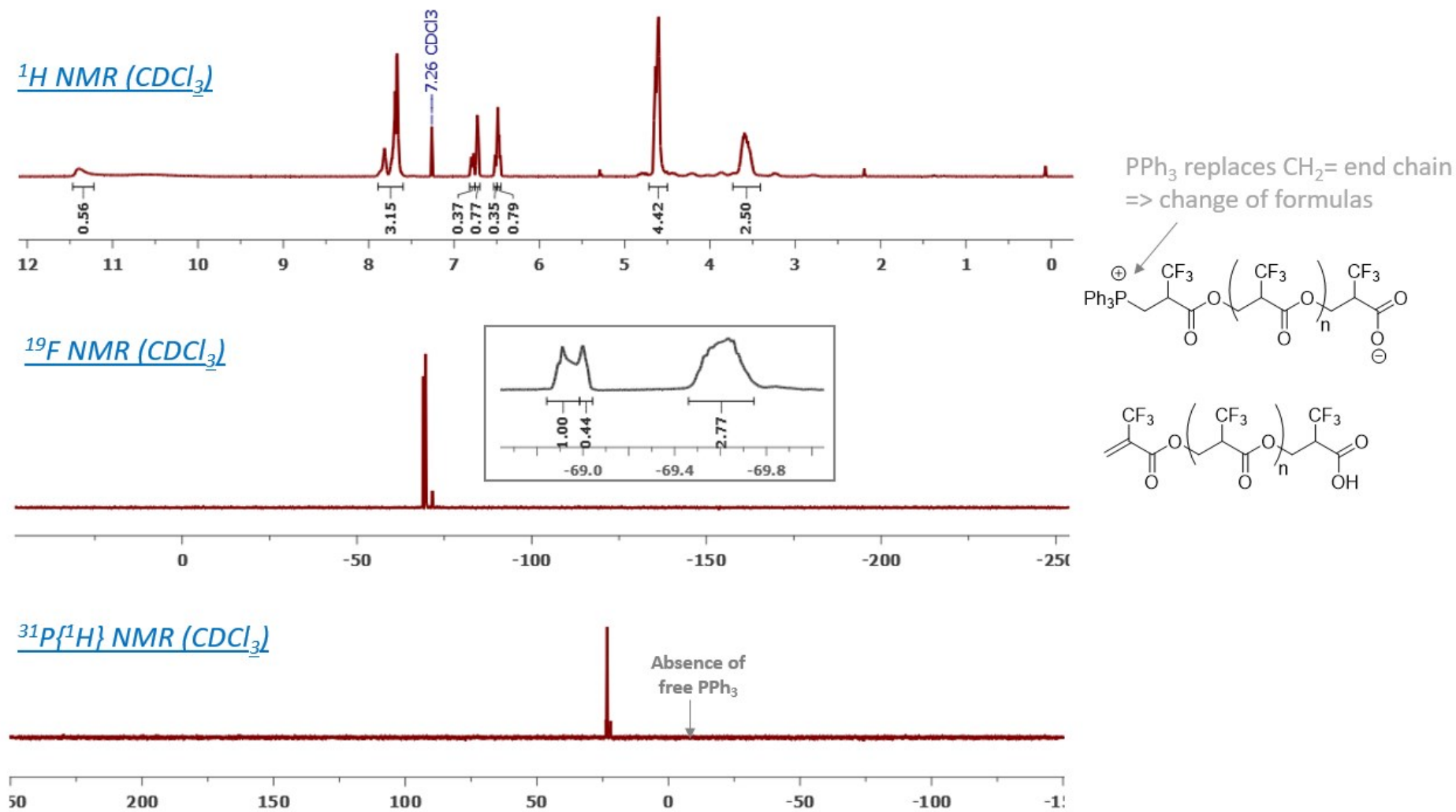
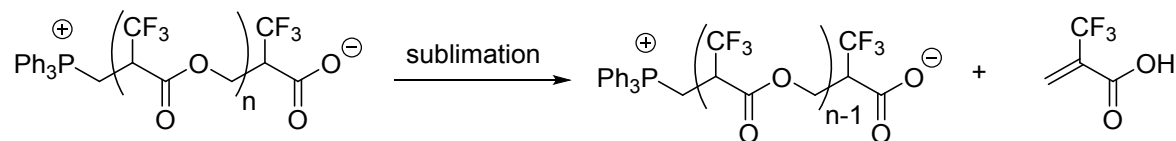


Figure S26 : ^1H (top), ^{19}F (middle) and $^{31}\text{P}\{^1\text{H}\}$ (bottom) NMR spectra (in CDCl_3) of oligoMAF and its phosphonium obtained from PPh_3 (5 mol% at 60 °C) (Entry 15 – Table 1)

The phosphines were not released at the end of the oligomerisation and replace the CH₂= end chains. It is necessary to take into account their protons in the formulas for calculating MAF conversions and DP_n from ¹H NMR spectra. The reaction using PPh₃ (5 mol% at 60 °C) (Entry 15 – Table 1) was taken as an example. PPh₃ bearing 15 protons, the formulas were modified as follows :

$$\text{Conv. (MAF) (\%)} = \frac{\int_{7.6}^{7.9} PPh_3 + \int_{6.7}^{6.8} CH(\text{oligomers}) + \int_{3.6}^{3.7} CH(\text{oligomers})}{\int_{7.6}^{7.9} PPh_3 + \int_{6.7}^{6.8} CH(\text{oligomers}) + \int_{3.6}^{3.7} CH(\text{oligomers}) + \int_{6.9}^{6.9} CH(\text{unreacted MAF})} \times 100 \quad (1')$$

$$\text{DP}_n = \frac{\int_{7.6}^{7.9} PPh_3 + \int_{6.7}^{6.8} CH(\text{oligomers}) + \int_{3.6}^{3.7} CH(\text{oligomers})}{\int_{7.6}^{7.9} PPh_3 + \int_{6.7}^{6.8} CH(\text{oligomers})} = 1 + \frac{\int_{3.6}^{3.7} CH(\text{oligomers})}{\int_{7.6}^{7.9} PPh_3 + \int_{6.7}^{6.8} CH(\text{oligomers})} \quad (3')$$



Scheme S2 : Retro-oxa-Michael addition observed when sublimating the phosphonium of oligoMAF

Water Contact Angle

Table S2 : Detailed measurements of contact angles and volume of the water drop on the oligoMAF surface, obtained with $P(C_6H_{11})_3$ (Entry 11 – Table 1)

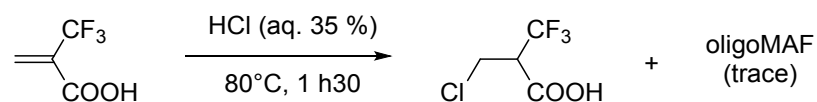
t (s)	CA(L)[°]	CA(R)[°]	Vol[μL]	CA(A)[°]
0	106.6	107.3	3.1	107.0
4	101.3	101.8	4.1	101.5
8	98.8	98.1	4.1	98.4
12	93.1	93.7	4.5	93.4

CA, L, R and M stand for contact angle, left, right and average, respectively

Preparation of ClCH₂-CH(CF₃)(COOH) (MAF-Cl)

Optimisation

Chlorination of MAF was attempted with the use of concentrated aqueous HCl 35 % solution. In the presence of 1.1 equivalents of HCl and after 1 h30 of heating at 80 °C, the desired product was formed with the ratio MAF : MAF-Cl = 7 : 3 (Entry 1 - Table S1). The *oxa*-Michael addition oligomers were afforded in trace quantity. Longer reaction times led to better MAF conversion to MAF-Cl (MAF : MAF-Cl = 1 : 9) but also enhanced the *oxa*-Michael polymerisation. As the reaction mixture is a liquid, distillation was attempted to separate the desired product. However, trace of MAF made the purification difficult. In the goal of complete the reaction, higher HCl loading and temperature were tried without any success. The optimal conditions were then using HCl 35 % (2.2 equiv.) at 80 °C for 1.5 h to get MAF conversion of 90%.



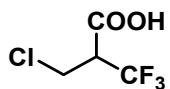
Scheme S3 : Preparation of MAF-Cl from MAF and HCl 35 % aqueous solution

Table S3 : Optimisation conditions for the preparation of MAF-Cl from addition of HCl onto MAF

Entry	Conditions	Time	MAF conversion (%)
1	HCl 35 % (1.1 equiv.), 60 °C	1.5 h	30
2		3 h	40
3		3 days	80
4	HCl 35 % (2.2 equiv.), 80 °C	1.5 h	90
5		18 h	90
6	HCl 35 % (3.3 equiv.), 80 °C	1.5 h	90

Procedure

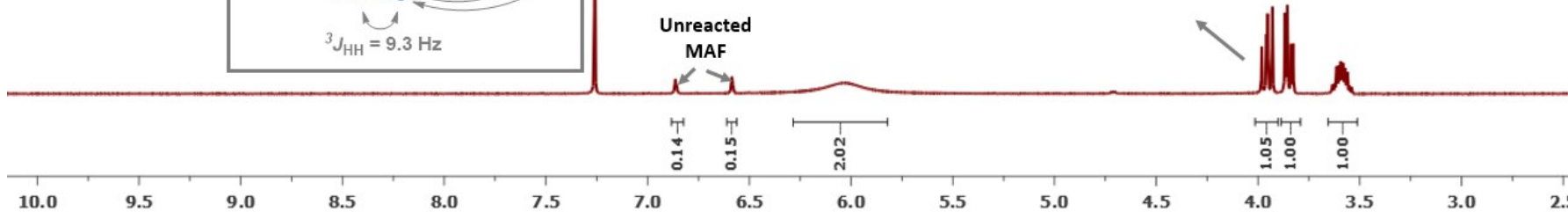
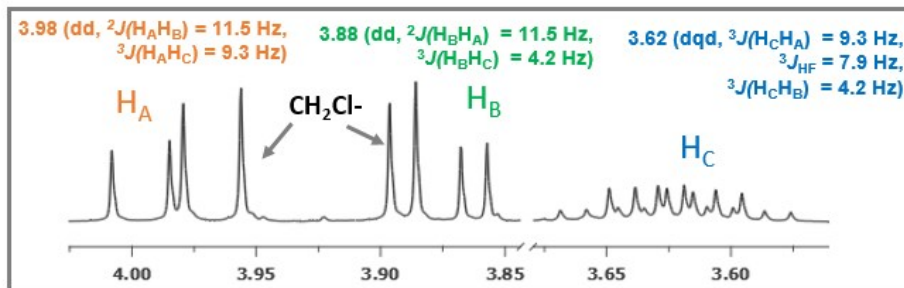
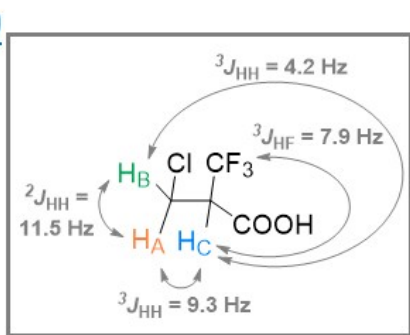
In a round bottom flask, were introduced MAF (7.00 g, 5 mmol, 1 equiv.) and HCl_{aq} 35% (13 mL, 14.5 mmol, 2.9 equiv.) under N₂ atmosphere. The mixture was heated to 80 °C for 3 h then cooled down to room temperature, extracted with dichloromethane and H₂O, dried over MgSO₄ and evaporated. A mixture of MAF-Cl (85 %) and MAF was obtained as a colorless liquid (6.3 g of mixture, equivalent to 5.5 g. of MAF-Cl, 63 % yield of MAF-Cl).



Chemical Formula: $C_4H_4ClF_3O_2$
 Molecular Weight: 176.52 g/mol
 Colorless liquid
 Boiling point : 75 °C (under 8.10^{-3} mbar)

1H NMR (400 MHz, $CDCl_3$) δ 3.98 (dd, $^2J_{HH} = 11.5$ Hz, $^3J_{HH} = 9.3$ Hz, 1H), 3.88 (dd, $^2J_{HH} = 11.5$, $^3J_{HH} = 4.2$ Hz, 1H), 3.62 (dq, $^3J_{HH} = 9.3$ Hz, $^3J_{HF} = 7.9$ Hz, $^3J_{HH} = 4.2$ Hz, 1H).
 ^{19}F NMR (377 MHz, $CDCl_3$) δ -70.07 (d, $^3J_{HF} = 7.9$ Hz)
 ^{13}C NMR (101 MHz, $CDCl_3$) δ 169.99 (s), 123.00 (q, $^1J_{CF} = 281.4$ Hz), 53.06 (q, $^2J_{CF} = 28.1$ Hz), 37.53 (q, $^3J_{CF} = 3.1$ Hz).

1H NMR ($CDCl_3$)



^{19}F NMR ($CDCl_3$)

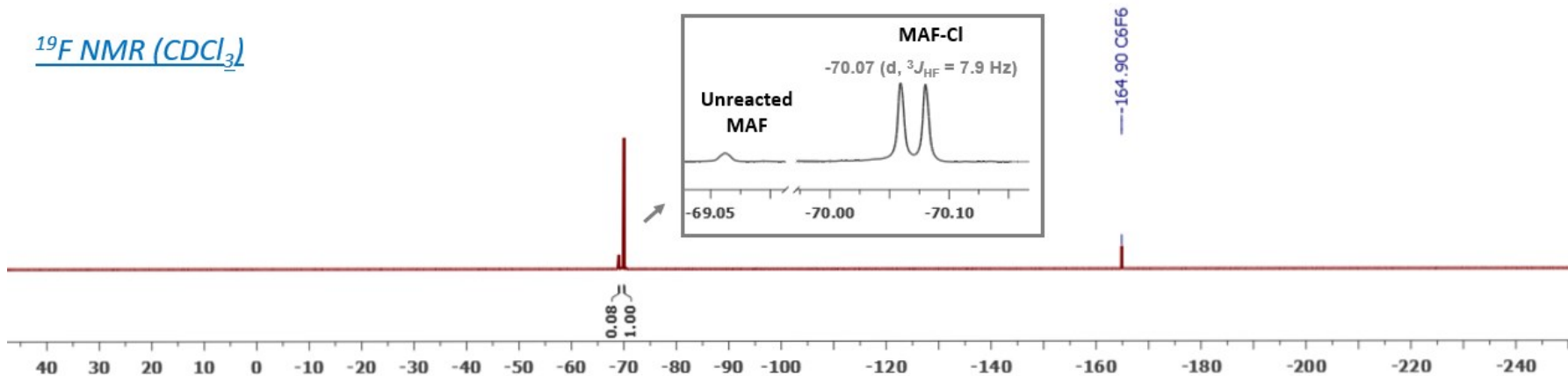
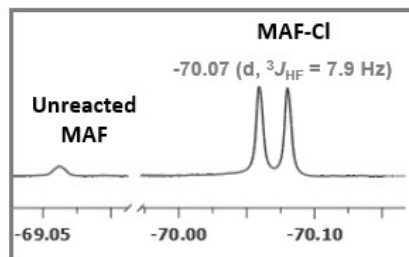


Figure S27 : ^1H and ^{19}F NMR spectra (in CDCl_3) of $\text{ClCH}_2\text{-CH}(\text{CF}_3)\text{COOH}$

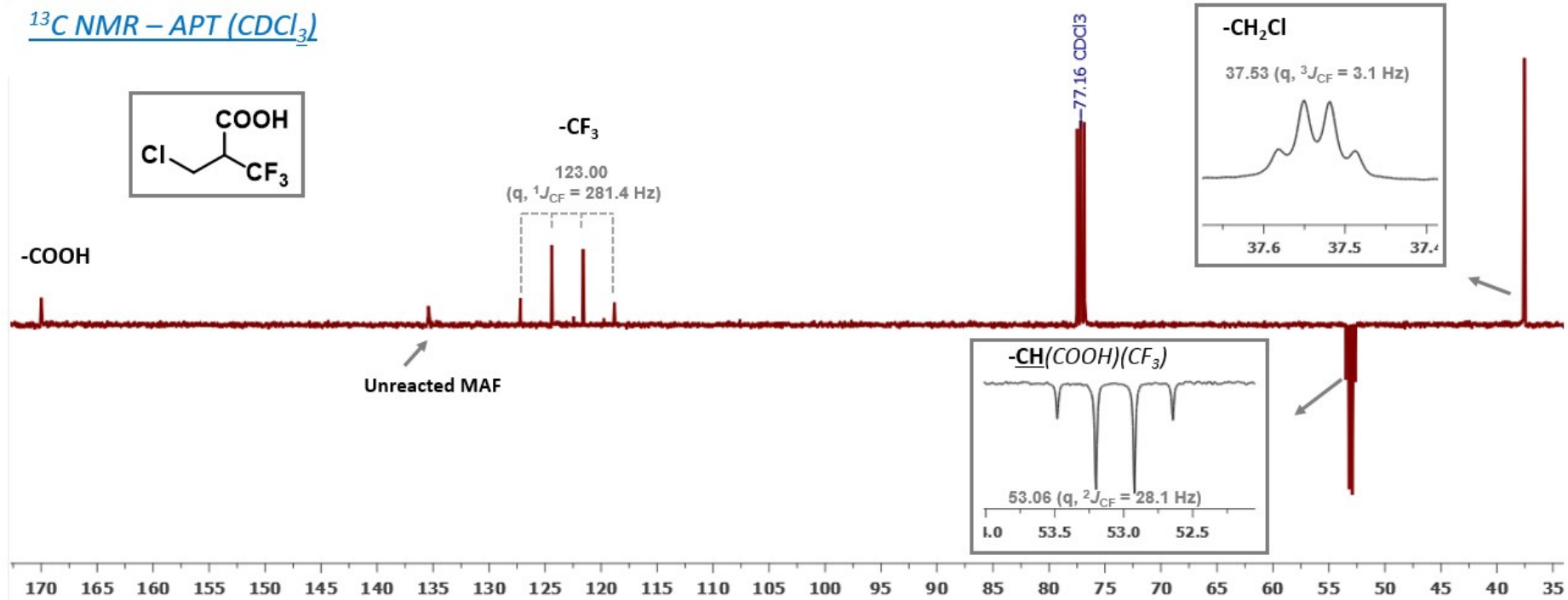
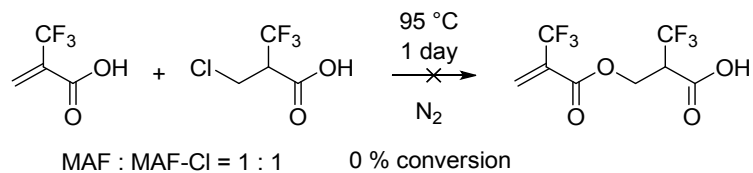
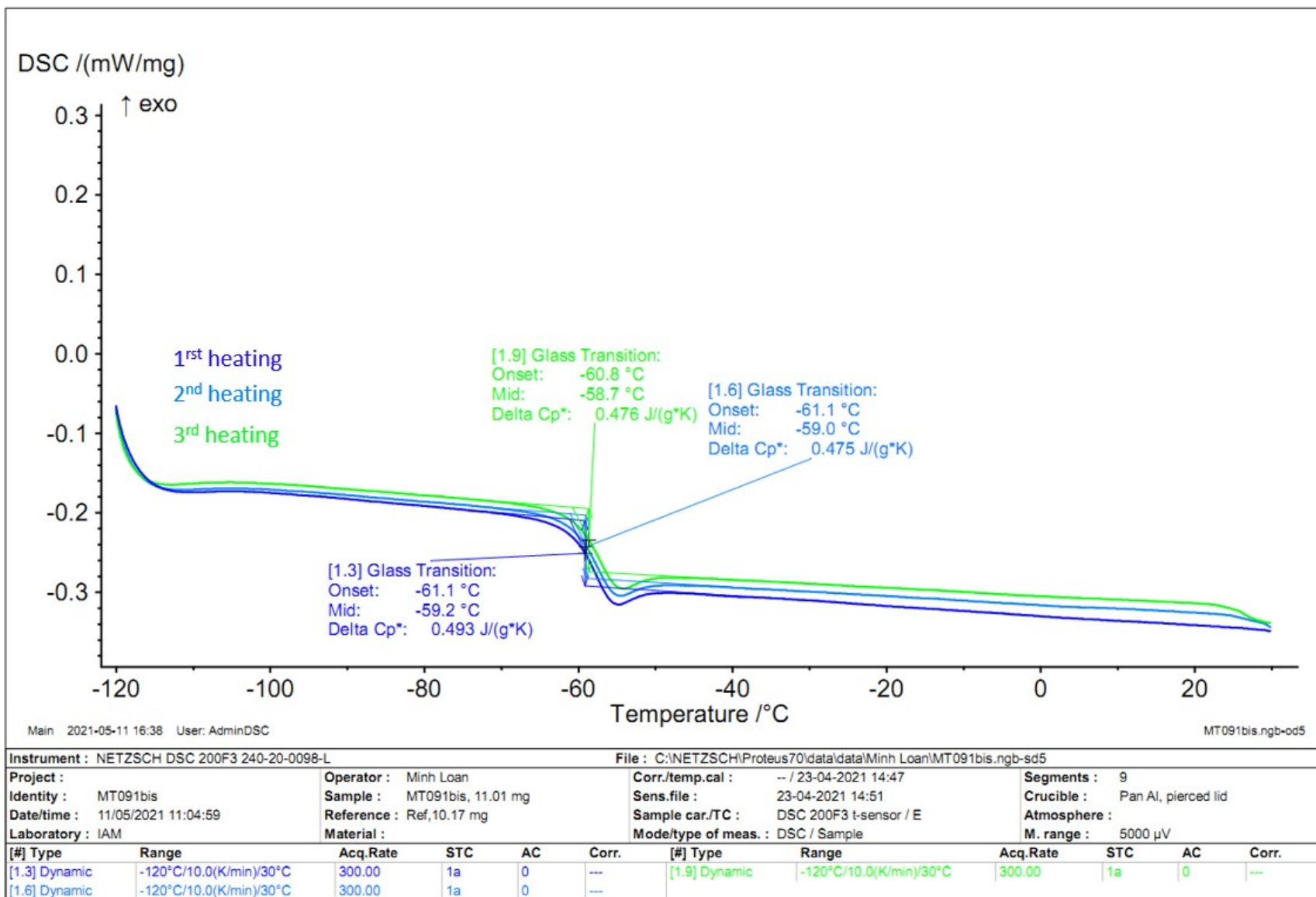


Figure S28 : $^{13}\text{C}\{^1\text{H}\}$ -APT NMR spectrum (in CDCl_3) of $\text{ClCH}_2\text{-CH}(\text{CF}_3)\text{COOH}$



Scheme S4 : Equimolar MAF and MAF-Cl mixture at 95 °C for 1 day



Created with NETZSCH Proteus software

Figure S29 : DSC thermogram of diMAF obtained without additive ($DP_n = 2.3$, Entry 1 – Table 1)

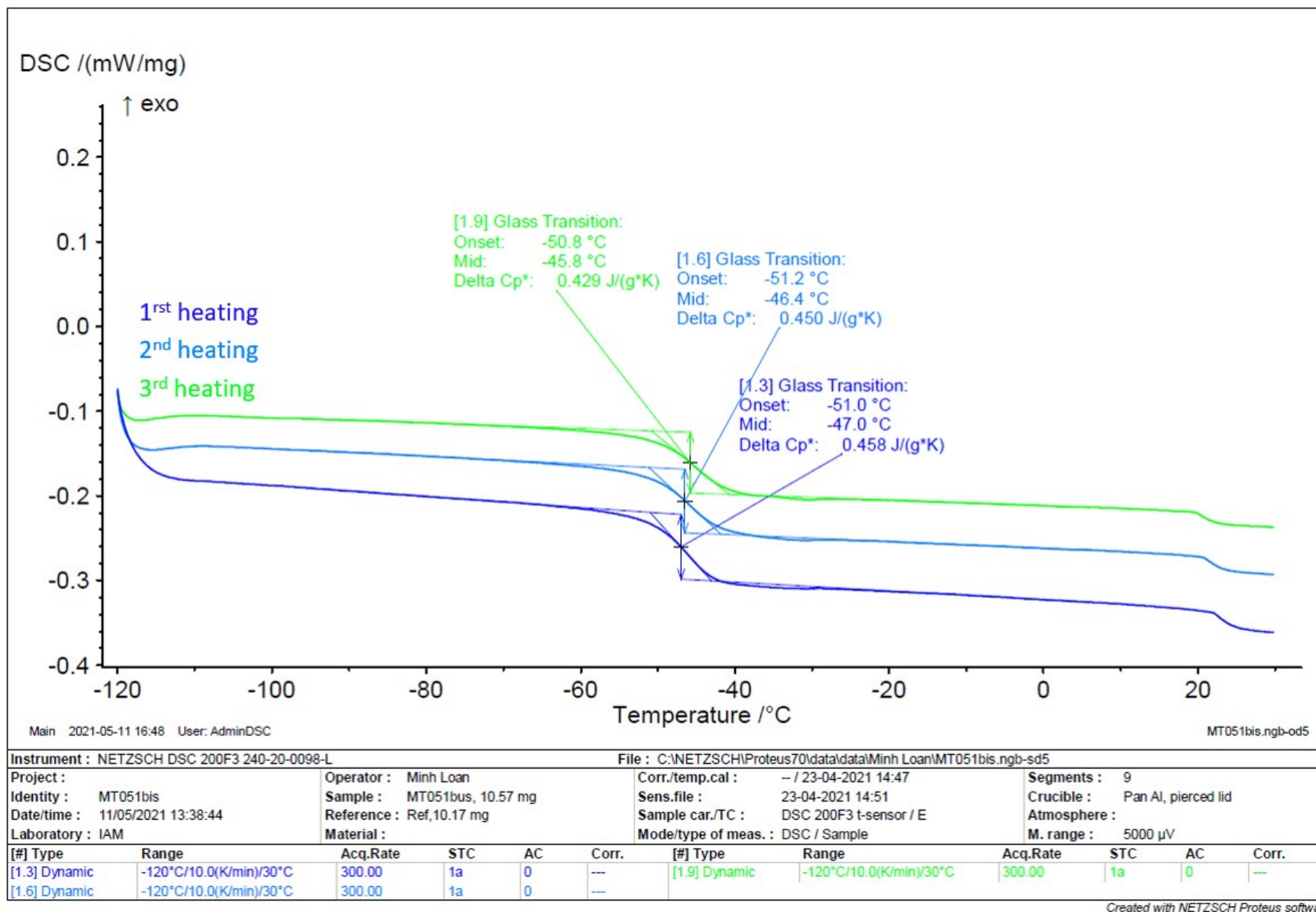


Figure S30 : DSC thermogram of oligoMAF obtained with DIPEA ($DP_n = 3.1$, Entry 9 – Table 1)

References

- (1) Lin, Z.; Guan, C.; Huang, L.; Wang, W.; Ling, Q.; Zhao, C. Catalysis Studies of Macroreticular Polystyrene Cation-Exchange Resin with Terminal Perfluoroalkanesulfonic Acids. *J. Chinese Chem. Soc.* **2013**, *60* (3), 261–266.
- (2) Pal, R.; Sarkar, T.; Khasnobis, S. Amberlyst-15 in Organic Synthesis. *Arkivoc* **2012**, *2012* (1), 570–609.